Vol. 29 (1998) *ACTA PHYSICA POLONICA B* No 12

QUANTUM CHAOS: ENTROPY SIGNATURES*

Paul A. Miller, Sarben Sarkar and Raphael Zarum

Department of Physics, King's College London
Strand, London WC2R 2LS, United Kingdom

(Received October 22, 1998)

A definition of quantum chaos is given in terms of entropy production rates for a quantum system coupled weakly to a reservoir. This allows the treatment of classical and quantum chaos on the same footing. In the quantum theory the entropy considered is the von Neumann entropy and in classical systems it is the Gibbs entropy. The rate of change of the coarse-grained Gibbs entropy of the classical system with time is given by the Kolmogorov–Sinai (KS) entropy. The relation between KS entropy and the rate of change of von Neumann entropy is investigated for the kicked rotator. For a system which is classically chaotic there is a linear relationship between these two entropies. Moreover it is possible to construct contour plots for the local KS entropy and compare it with the corresponding plots for the rate of change of von Neumann entropy. The quantative and qualitative similarities of these plots are discussed for the standard map (kicked rotor) and the generalised cat maps.

PACS numbers: 03.65.–w, 05.40.+j, 05.45.+b

1. Introduction

It is now well-known that non-linearity in classical systems generically leads to chaotic behaviour. This is usually defined as sensitive dependence on initial conditions for orbits. Within this context the quantum analogue does not exist. We will summarise our approach to this problem and then expand on the issues as we proceed. Classical and quantum mechanics, however, are not very different when the dynamics of classical systems is rephrased in terms of the linear Liouville equation for phase space distributions. The sensitive dependence on initial conditions is mirrored, in this formulation, by the linear increase with time of the coarse-grained Gibbs entropy which is also known as the Shannon entropy. A highly artificial but

* Presented by S. Sarkar at the XXXVIII Cracow School of Theoretical Physics, Zakopane, Poland, June 1–10, 1998.

simple model illustrates this point effectively. The tent map is a chaotic map and a geometrically related map is the modulus map:

$$x_{n+1} = 2x_n \mod 1\,. \tag{1}$$

The action of this map is most easily seen in the binary representation. Given a binary representation of an initial condition, the map moves the "decimal" point at each iteration one point to the right and drops all digits to the left of the point. Clearly if two initial points differed first at the nth "decimal" digit, then after n iterations there is a large difference between the iterates. To retain a certain accuracy the number of digits required for the specification of the initial state increases as n. Missing information is Shannon entropy and it increases linearly with n or time. More formally we can partition phase space into cells $\{C\} = \{C_1, C_2, \cdots, C_p\}$. Iterates of a map can be expressed as symbol sequences $j_0, j_1, \cdots, j_{n-1}$ say. If the probability of such a sequence is $p\,(j_0, j_1, \cdots, j_{n-1})$ then the dynamical Shannon entropy per unit time $H\,(\{C\})$ is defined to be

$$H\,(\{C\}) = -\operatorname*{Lim}_{n\to\infty} \frac{1}{n} \sum_{j_0,\cdots,j_{n-1}} p\,(j_0, \cdots, j_{n-1}) \log p\,(j_0, \cdots, j_{n-1})\ . \tag{2}$$

In terms of $H\,(\{C\})$ the Kolmogorov–Sinai entropy h_{KS} is defined as

$$h_{\mathrm{KS}} = \sup_{\{C\}} H\,(\{C\})\ . \tag{3}$$

h_{KS} measures the average information per iteration needed concerning the input in order to maintain the accuracy of the output. This sensitivity to initial conditions can be reexpressed in terms of entropy through the Alekseev–Brudno theorem:

$$h_{\mathrm{KS}} = \sum \Lambda^{+}, \tag{4}$$

where the Λ^{+}s are the positive Lyapunov exponents. The von Neumann entropy S is defined by

$$S = -\mathrm{Tr}\,(\rho \log \rho)\,, \tag{5}$$

ρ being the density matrix of the system. For a Hamiltonian system unitary evolution implies

$$\frac{d}{dt} S = 0 \tag{6}$$

and so S is not a dynamical entropy. An ingredient which is crucial in quantum mechanics is measurement. Classically measurement on a system can be made such that there is an arbitrarily small disturbance on the system.

In quantum mechanics this is not the case as can be appreciated from the Heisenberg uncertainty relations. Already a decade ago, Sarkar and Satchell [26] discussed the possible role of environment in the quantum evolution of chaotic systems. This line of thought suggests that a more natural way to restore the quantum classical correspondence is to consider physical systems not as being isolated from the rest of the universe but as undergoing constant and varied interactions with it. This is an inescapable fact of life and must be accounted for, at least approximately, in any attempt to describe the *real* quantum behaviour of microscopic and macroscopic objects [11, 12, 15].

The destruction of phase coherence in a quantum system because of the continuous monitoring of its state by internal [16] and external [11,12,15,17, 18] degrees of freedom is a process known as *decoherence*. Correlations are established when initially noninteracting subsystems — the system and its environment — begin to interact. The subsequent loss of information from the system to the environment results in a reduction in the interference effects present in the system. Exactly the same situation arises if we try to determine the slit through which a photon or a particle travels in a double-slit experiment: interference effects on the screen are lost if we, the observers, acquire information about which slit is used at any one time.

As an example let us consider a system coupled to an environment through its position coordinate. It will be influenced in the following way [17]: if the self-Hamiltonian of the system is ignored the eigenstates of position will not evolve at all and will not be influenced directly by the environment. The position eigenstates are then known as *pointer states*. However, *superpositions* of these pointer states can be shown to decay rapidly into mixtures of position eigenstates. So, even though the superposition principle of quantum mechanics states that every state in the Hilbert space spanned by these pointer states can exist in principle, interaction with an environment effectively selects certain states — the pointer states — as being the most stable and reduces all coherent superpositions of these states to incoherent mixtures.

This process, an *environment-induced superselection rule* [17], can be generalised to more realistic situations in which the self-Hamiltonian of the system is important. It is, of course, then unlikely that any state will ever be absolutely free from environmental influence and the criteria for the pointer states changes from absolute stability to the *greatest* stability instead, *i.e.* pointer states will be defined as those least prone to deterioration into a mixture. This can be quantified using the von Neumann entropy of the reduced density matrix of the system [17, 19]. A set of *preferred* states is then defined as the set of states which are most stable, *i.e.* those for which the entropy increases most slowly, in a procedure known as the *predictability sieve* [17, 19].

2. Inverted harmonic oscillator

In a rigorous examination of the entropy approach to the correspondence problem Zurek and Paz [11] have considered the completely tractable model of an inverted harmonic oscillator coupled to a high temperature (harmonic) bath. The inverted oscillator Hamiltonian takes the form

$$H(p,q) = \frac{p^2}{2} - \frac{\Lambda q^2}{2}, \tag{7}$$

so the potential energy function is an inverted parabola with its apex at the origin. It is a model of instability in classical mechanics and the phase space dynamics governed by this Hamiltonian is an excellent model of a hyperbolic fixed point [8]. It is certainly *not* a chaotic system — it lacks the folding required — but the parameter Λ is analagous to a Lyapunov exponent in a genuinely chaotic system. This is because it induces the exponential rate of divergence (convergence) of nearby points on the unstable (stable) manifold in its 2-dimensional phase space. These linear manifolds intersect at the origin, *i.e.* at the only fixed point of the dynamics.

Let us consider the time evolution of a particle moving in the inverted oscillator potential $V(q) = -\Lambda q^2/2$, but now let us also consider it to be coupled through its position q to the position variables of each oscillator in the infinite set which we use as a model of a thermal bath at a high temperature. Further choosing the distribution of frequencies of this set to be of an Ohmic type [18] it is possible to derive a master equation for the reduced density matrix, ρ_q, which describes the state of the particle at any time. In the position representation it reads [12, 20]

$$\frac{\partial \rho_q}{\partial t} = \frac{1}{i\hbar}\left[H, \rho_q\right] - \gamma(x-y)\left(\frac{\partial}{\partial x} - \frac{\partial}{\partial y}\right)\rho_q - \frac{D}{\hbar^2}(x-y)^2\rho_q, \tag{8}$$

with $D := 2m\gamma k_B T$ and where γ both describes the strength of coupling to the environment and serves as a dissipation parameter. Upon making the weak coupling assumption of $\gamma \ll 1$, Zurek and Paz [11] have solved the equation corresponding to the above for the Wigner function. This task is made considerably easier by the fact that the form of the potential for the inverted oscillator implies that all the quantum correction terms vanish identically and the equation becomes

$$\frac{\partial W}{\partial t} = -\Lambda q\frac{\partial W}{\partial p} - p\frac{\partial W}{\partial q} + D\frac{\partial^2 W}{\partial p^2}. \tag{9}$$

Here $D = 2\gamma k_B T$ now, since $m = 1$ is chosen for the particle in the inverted oscillator potential. More generally, 3rd or higher order derivatives of $V(q)$ would appear in Eq. (9).

On calculating the rate of change of von Neumann entropy it can be shown that [11]

$$\frac{dS}{dt} \approx \Lambda \left(1 + ae^{-2\Lambda t}\right)^{-1} \to \Lambda, \tag{10}$$

as $t \to \infty$. Here a is a constant dependant on the initial choice of density matrix.

2.1. The Zurek and Paz conjecture

Zurek and Paz [11,12,15] noticed the strikingly different rates of entropy increase between positive and zero Λ. They proposed to solve the correspondence problem and conjectured that the rate of entropy production in a quantum system weakly coupled to a high temperature environment can be used as a test to determine the nature of the Hamiltonian evolution of that system — quantum and classical. Quantitatively, Eq. (10) becomes the conjecture when Λ is replaced by the sum of the positive Lyapunov exponents. Classical unpredictability would then imply unpredictability in its weakly perturbed quantum counterpart.

This conjecture is supported by the fact that hyperbolic points, such as that exhibited at the origin in the inverted oscillator model, are ubiquitous in the phase space of a chaotic system [4]. (Resonant tori become alternating sequences of elliptic and hyperbolic points upon the introduction of slight perturbations.) The inverted oscillator model is, therefore, a possible representation of the *local* behaviour in chaotic classical evolution.

An important appeal of this conjecture is the identification of the averaged sum of the positive Lyapunov exponents in a d-dimensional system with the *Kolmogorov–Sinai* (KS) or *metric* entropy, h_{KS}, (*cf.* Eq. (4)) of classical chaos theory [5,60,64]. h_{KS} is commonly used as a means to define a system as being classically chaotic. If $h_{\mathrm{KS}} > 0$ we say the system is chaotic and if $h_{\mathrm{KS}} = 0$ we say it is regular.

3. Criticisms of the Zurek and Paz approach

The Zurek and Paz conjecture as expressed in equation (10) has been arrived at with the help of various simplifying assumptions. In this section we will endeavour to catalogue these assumptions. We will also make some general criticisms of the Zurek and Paz approach.

3.1. A catalogue of assumptions

There are a number of reasons why we should question any conjecture regarding the entropy production of an open quantum analogue of a genuinely chaotic system based on so simple a picture as that presented above.

The quantitative framing of the conjecture in equation (10) would, one suspects, be the first casualty in any real system. Moreover, a more qualitative version of the conjecture, *i.e.* the conclusion that open quantum systems will produce entropy at a rate which is merely *an increasing function* of some measure of the chaos in their classical analogue, could also be in jeopardy.

3.1.1. Model-dependent assumptions

The first criticism has to do with the fact that although the quantum corrections to the classical Liouville term in the evolution equation for the Wigner function may be limited upon the introduction of the environmental diffusion term, they are, nonetheless, always present. The quadratic nature of the inverted oscillator potential cannot take this effect into account since derivatives of third and higher order vanish, and with them the quantum corrections. To illustrate the relevance of this fact we note that Farini *et al.* [22] have shown that the presence of even small quantum corrections can lead to increasing differences between quantum and classical phase space distributions as they evolve in time.

In addition, the conjecture was made on the basis of a partial differential equation for the Wigner function, an equation from which the dissipation term was dropped. The mathematical justification for this procedure was to let the dissipation parameter $\gamma \to 0$ while keeping $D = 2m\gamma k_B T$ constant. This means, essentially, increasing the environmental temperature and/or the mass of the particle. But here, as with the first point, we must stress that the dissipation term can *never* be dropped completely since this would entail setting $\gamma = 0$ identically, implying decoupling from the environment and hence $D = 0$ too. Thus, there will always be some dissipation in the system, however small. We will directly address this problem below and will present an exact expression for the rate of entropy increase of an open inverted oscillator when this approximation is not made. The result generalises equation (10) in that it explicitly reveals the influence of the dissipation parameter on the entropy production rate.

A third and related model-dependence centres on the choice of a thermal bath as an environment. Assumed are such features as a very large or even infinite number of degrees of freedom in the bath, the special choice of the density of frequencies of the oscillators which comprise it and the independent, non-interacting nature of these oscillators.

3.1.2. Phase space considerations

How well does the inverted oscillator model the phase space dynamics of a genuine chaotic system? Zurek and Paz [11] contend that it is a faithful representation of the *local* dynamics seen by an evolving trajectory in phase

space. However, the inverted oscillator model is not chaotic. It has fixed stable and unstable directions which intersect at the origin of phase space, the *only* fixed point of the dynamics. Thus, it does not take into account the effect of elliptic points, homoclinic points, heteroclinic points, stable islands or cantori on the open quantum dynamics [1, 4]. In short, it is not a good model of the extremely complex mixed phase spaces in which trajectories of generic Hamiltonian systems evolve.

Importantly, too, the inverted oscillator model does not take into account the *folding mechanism* which, along with stretching, characterises classical chaos [1, 4]. Indeed, the fixed direction of the stable and unstable manifolds are quite inadequate to represent the rapid change in the direction of the local stable and unstable manifolds typically seen in genuinely chaotic systems. In ignoring this essential ingredient of chaos one is, in effect, ignoring the fact that the directions of squeezing and contraction change rapidly along a typical trajectory.

Farini *et al.* [22] have illustrated the dangers of ignoring the folding effect by studying a driven particle in a quartic double well potential *in the absence of an environment* (see [13] for a study *with* an environment). By focusing on a chaotic parameter regime in which the directions of the stable and unstable manifold change rapidly they have defined a new timescale, τ_{twist}, as the inverse of the average twisting frequency of these changes in direction. Moreover Zurek and Paz [11,12] have defined a timescale on which the quantum corrections can be expected to become at least as significant as the classical term in the evolution of the Wigner function where the quantum corrections involve spatial derivatives of the potential. The quantum evolution of an initial coherent state can be compared to an initial classical Gaussian distribution of points in phase space. At every point in a chaotic region of phase space there are are local stable and unstable directions along which neighbouring trajectories will either exponentially contract or expand, respectively. In addition, the exponential rate at which both these processes occur is governed by the local Lyapunov exponents. Conservation of volume in phase space, however, requires that for every positive exponent, Λ, corresponding to an unstable direction there is a negative exponent, $-\Lambda$, corresponding to a stable direction. Thus, for a "small" $\hbar$ the initial quantum state will evolve in this classical manner: exponentially expanding in the unstable directions but exponentially contracting in the stable ones. Now at any point in phase space there will exist directions corresponding to stable and unstable evolution. In general these directions will always have nonzero projections onto the coordinate axes. If we consider any stable direction associated with a Lyapunov exponent $-\Lambda$, then a wave packet will contract along the momentum coordinate, p say, according to

$$\Delta p(t) = \Delta p(0) \exp(-\Lambda t), \tag{11}$$

where $\Delta p(t)$ defines the variance in that momentum direction at a time t. Of course, the uncertainty $\Delta q(t)$ in the position q conjugate to p must obey

$$\Delta q(t)\Delta p(t) \geq \frac{\hbar}{2} \tag{12}$$

and so

$$\Delta q(t) \geq \frac{\hbar}{2\Delta p(0)} \exp(\Lambda t). \tag{13}$$

If the potential $V(q)$ is sufficiently nonpathological it should always be possible to make a harmonic approximation to it locally. So, if the extent of the Wigner function in every direction q remains sufficiently small we will always have negligible quantum corrections since $\partial^m V(q)/\partial q^m = 0$ $\forall m \geq 3$ when the harmonic approximation to $V(q)$ applies. However, when the wavepacket spreads coherently in position until the harmonic approximation no longer applies this picture is changed irrevocably.

We define first a lengthscale on which the potential is no longer quadratic,

$$\chi := \sqrt{\frac{\partial_q V}{\partial_q^3 V}}, \tag{14}$$

i.e. χ^2 is the ratio of the usual classical force and a term in the first significant nonlinear correction to appear in the evolution equation for the Wigner function. Note that $\chi \to \infty$ as $\partial_q^3 V \to 0$. From equation (13) we see that $\Delta q(t)$ reaches this scale at certain time $t_\hbar$ given by

$$t_\hbar := \frac{1}{\Lambda} \ln\left(\frac{2\Delta p(0)\chi}{\hbar}\right). \tag{15}$$

This is approximately the time at which the quantum corrections will become nonnegligible, for *any* value of $\hbar$. They then proceed to classify the chaotic dynamics in the following way: if $t_\hbar \leq \tau_{\text{twist}}$ it means that the directions of the stable and unstable manifolds remain constant for long enough to allow the quantum correction terms to become as large as the classical Liouville term. The dynamics will then be flagrantly quantum. If, on the other hand, $t_\hbar \gg \tau_{\text{twist}}$, one expects that the rapid change in the directions of expansion and contraction will curtail the growth of the quantum correction terms. The dynamics should then mimic the classical Liouville flow for times in excess of $t_\hbar$. Indeed, this is what they have found [22]: when $t_\hbar \gg \tau_{\text{twist}}$ they find the quantum correction terms to be very much smaller than the Liouville terms, even when $t > t_\hbar$. They warn, however, against defining quantum-classical correspondence as a small ratio of the former to the latter. For, even when this is the case, they still find an appreciable difference between the quantum and classical distributions, one, indeed, which grows in time.

We shall later address these issues by examining the effect that a mixed phase space, complete with all the complexity and folding we might expect, has on the rate of entropy increase.

Finally, we note that the inverted oscillator model cannot account for the special *dynamical localisation* behaviour seen in many studies of quantum chaos since its inception [7, 9].

4. A reexamination of the inverted oscillator

4.1. Generalised approach

So far we have given an outline of the reasons for an environmental approach to the study of classically chaotic quantum systems. In particular we concentrated on the central thesis of Zurek and Paz that the behaviour of a quantum system in contact with an environment can provide a good indication as to the nature of the analagous classical, Hamiltonian evolution.

The appeal of equation (10) is great, as we have discussed, since, through the classical KS entropy, it directly relates the rate of information production in an open quantum system to that in its classically chaotic counterpart. It indicates that the more chaotic a classical system is then the more quickly will we lose information about the state of the quantised system to a (weakly) perturbing environment. We previously pointed out some weaknesses of this model. By implication, therefore, there is no *a priori* reason to believe in the direct applicability of the quantitative conjecture of equation (10) to a typical classically chaotic quantum system.

We have [23] generalised the calculation to thermal baths with arbitrary temperatures and obtained

$$\begin{aligned} \frac{dS}{dt} &\overset{t\to\infty}{=} \kappa - \gamma \\ &= \kappa' , \end{aligned} \tag{16}$$

where the shorthand definition

$$\kappa = \sqrt{\Lambda^2 + \gamma^2} \tag{17}$$

has been used here. This result gives the asymptotic rate of entropy increase in situations where energy dissipation is important and cannot be neglected. As γ determines the strength of the coupling to the environment we can now see that the rate at which an unstable, possibly chaotic system will lose information to the environment can in fact depend on the coupling strength [15]. Note, however, that this asymptotic rate does reduce to the

asymptotic rate found previously in the weakly coupled regime

$$\begin{aligned} \frac{dS}{dt} &\overset{\kappa t\to\infty}{=} \sqrt{\Lambda^2+\gamma^2}-\gamma \\ &\approx \Lambda, \quad \text{when } \gamma \ll \Lambda, \end{aligned} \tag{18}$$

as required.

4.2. Concluding remarks

We have used the inverted harmonic oscillator to model instability in open quantum systems and have found that the rate of increase of the von Neumann entropy depends, for large times, on the degree of instability in the system *and* on the strength of interaction with the environment in a simple way. In fact, in deriving equation (16) we have generalised the result of Zurek and Paz to the case of *finite* dissipation. The purpose of studying such an elementary system is to build up some degree of intuition concerning the behaviour of quantum chaotic systems coupled to an environment. However, and as we have already discussed, *a priori* claims as to the applicability of predictions based on an analysis of the inverted oscillator to classically chaotic quantum systems should be treated with caution. Similarly, the result of equation (16) which, we recall, has been derived for arbitrary temperatures, does *not* mean that we can expect the von Neumann entropy of a genuinely chaotic system to increase at the given rate at all temperatures. This is because the quadratic nature of the inverted oscillator potential implies that the quantum corrections which arise in the evolution of the Wigner function, vanish identically. In general, however, they do *not* vanish for genuinely chaotic systems. It is precisely these corrections which lead to the breakdown in phase space correspondence at the time $t_\hbar$ given by equation (15). If the temperature is not high enough then the phase space behaviour will be flagrantly quantum after $t_\hbar$ and equation (16) will then not hold. Once again, therefore, the quadratic nature of the inverted oscillator potential makes it dangerous to extrapolate to genuinely chaotic systems.

5. Model chaotic systems

It seems, therefore, that taking the effect of an environment into account helps to re-establish the correspondence between quantum and classical mechanics [17, 18]. It is entirely natural, then, to apply it to situations where the problem is most evident; namely, the quantum behaviour of classically chaotic systems [11, 12].

Before we can continue with our discussion we need to consider models which will generically embody the features of classical chaos. We will

consider first the large class comprising Hamiltonian systems. The orbits in chaos are very complicated and so it is natural to diminish the complexity of the description of orbits by considering Poincaré sections. This naturally leads onto area-preserving maps. An important class of such maps are twist maps which arise for integrable tori and are deformed by non-integrable perturbations. In action-angle variables

$$\begin{aligned} \phi' &= \phi + \partial_{I'} S_0\left(I'\right) + \varepsilon \partial_{I'} S_1\left(I', \phi\right) , \\ I' &= I + \varepsilon \partial_{\phi} S_1\left(I, \phi\right) . \end{aligned} \tag{19}$$

An important example of such a twist is the so called standard map:

$$\begin{aligned} \phi' &= \phi + I' \mod 1 \\ I' &= I - \frac{K}{2\pi} \sin\left(2\pi\phi\right) . \end{aligned} \tag{20}$$

This map can also be thought of as Hamilton's equations for the following time-dependent Hamiltonian:

$$H\left(I, \phi, t\right) = \frac{I^2}{2} - \frac{K}{4\pi^2} \cos\left(2\pi\phi\right) \sum_{n=-\infty}^{\infty} \delta\left(t - nT\right) . \tag{21}$$

The quantisation of this Hamiltonian follows by making ϕ and I operators with canonical commutation relations. The δ-function kick is not strictly necessary although we find it a convenient formalism. In fact it is possible to consider a related Hamiltonian which leads to the same one step dynamics, viz.

$$H\left(I, \phi, t\right) = \begin{cases} \frac{I^2}{2\gamma} & 0 < t < \gamma T \\ \frac{K}{4(\gamma-1)\pi^2} \cos\left(2\pi\phi\right) & \gamma T < t < T \end{cases} \tag{22}$$

for $0 < \gamma < 1$. It is now important to characterise classical chaos in such models in some detail. The (I, ϕ) notation is now replaced by (p, q) to highlight the momentum (p) and position (q) variables in classical phase space.

5.1. The onset of chaos

We will employ the standard map (21) to describe, in terms of orbits, the onset of chaos and to elucidate the range of phenomena which occur as a result. The following subsections are organised by increasing levels of chaotic behaviour with figure 1 showing the sequence of phase space plots for increasing K.

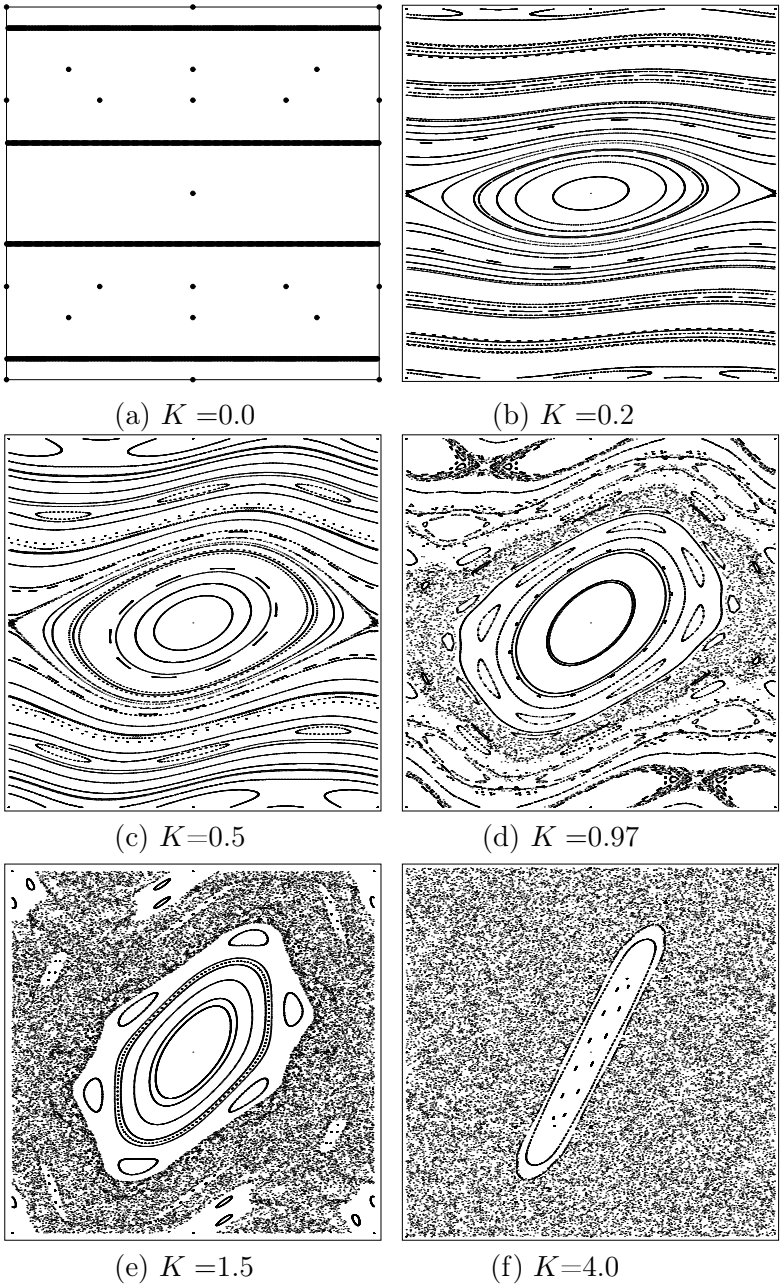

(a) K =0.0 (b) K =0.2

(c) K=0.5 (d) K =0.97

(e) K =1.5 (f) K=4.0

Fig. 1. Phase space of the classical standard map with varying K values bounded on the interval $[-\frac{1}{2}, \frac{1}{2})$ for both q and p.

5.1.1. The integrable case

We begin at $K = 0$ when the standard map becomes $p_{n+1} = p_n$, $q_{n+1} = q_n + p_{n+1}$, (mod $q = 1$). Thus p_n is a constant of the motion, and q_n grows at a constant rate depending on p_n. The solution is $p_n = p_0$; $q_n = q_0 + np_0$ and thus the map is integrable. The *frequency* is defined, if it exists, as the limit

$$\omega = \lim_{n\to\infty} \frac{q_n - q_0}{n}. \tag{23}$$

Trivially, when $K = 0$, $\omega = p_0$, for any initial condition. For each rational ω, $p_0 = n/m$ (where n, m are positive integers) and the (n, m) orbit is periodic with period m. Rational values of ω occur as a dense set of values of $p_0 = n/m$.

However, almost all points have an irrational ω so that the orbit never returns to its initial condition. Thus when $K = 0$, the standard map is termed *quasiperiodic* because even when ω is irrational the orbit is *recurrent*, *i.e.* it returns arbitrarily close to its initial condition with the q co-ordinate densely covering the line $p =$constant on the unit square in phase space. On the other hand, the orbit for a rational ω forms a finite set of periodic points. The phase space of this integrable map is shown in figure 1(a). Since the standard map is periodic in q, these lines across the phase space actually represent circles. Both the continuous circle of points associated with an irrational ω orbit and the discrete circle of points associated with a rational ω orbit are called *rotational invariant circles*. It is "rotational" because it encircles the unit phase space in the q direction. More generally, these rotational invariant circles become (N-dimensional) *rotational invariant tori* in an integrable system with an N-dimensional phase space.

5.1.2. Nearly integrable case

Figure 1(b) shows how much of the structure of the integrable map persists as K is increased from zero. The fact that most of the irrational ω orbits still seem to lie on (densely filled) rotational invariant tori is a prediction of the Kolmogorov–Arnol'd-Moser theorem [55], thus they are called KAM tori.

However, there are clearly another class of orbits which we see by focusing on the points of rational frequency. For example, near $p = 0$, where there is a circle of points of frequency 0/1, figure 1(b) shows an "island." This consists of a family of curves that are circles, but do not span unit phase space. These are *librational*, as opposed to rotational, circles and as before become N-tori in higher dimensions. The island is bounded by a *separatrix*, which is a curve separating the librational and rotational tori. The region of phase space bounded by the separatrix is called a "resonance zone" or simply

a resonance. The island is *not* reflection symmetric about the p axis, and be begins to distort as K is increased.

There are also resonances for other rational values of p, corresponding to the periodic orbits with frequencies n/m. Each resonance consists of a chain of m islands, several of which are shown in figure 1(c). At the centre of each island, and at the cusp of the separatrix, there are periodic orbits with frequency n/m. Orbits trapped in an island move successively from one island to another, following the periodic orbit, skipping over $n-1$ islands with each iteration of the mapping. There are thus entire regions of phase space each having a different frequency n/m. These are segregated by the KAM tori. Chaotic trajectories make up the narrow (fuzzy) bands at the resonance borders.

5.1.3. Transition to chaos

As K increases, the resonances grow in size, and the region of phase space occupied by rotational invariant KAM tori necessarily shrinks. KAM tori are destroyed when resonances engulf the region of phase space they once occupied. Figure 1(d) shows the standard map at a chaos parameter value for which many of the KAM tori are destroyed. All the resonances are becoming increasingly distorted by the large central resonance.

It has been shown that when K is large enough there can be no KAM tori [56]. Greene [57] discovered that for the standard map, the last KAM torus to be destroyed has frequency equal to the golden mean ($\omega_{\text{last}} = (1+\sqrt{5})/2$) and occurs for $K_{\text{last}} \approx 0.97$. We show the phase space for the standard map with this chaos parameter in figure 1(e).

The islands are *fractal* in that around each one are smaller similar islands and around each of these are even smaller similar islands [58]. The fact that all islands have satellite islands on ever smaller scales testifies to the complexity or fractality of the phase space.

5.1.4. Global chaos

In figure 1(e) the last remaining KAM torus, which stretches horizontally across the unit phase space, is broken. When $K \leq 0.97$ it is not possible for any trajectories to diffuse vertically through this line and reach arbitrarily large values of p. But beyond this K value the map becomes globally chaotic in that chaotic trajectories can reach *all* regions of phase space. The remaining resonances contain small stable islands in a chaotic sea of trajectories. Figure 1(f) shows the standard map for $K = 4$ when most of the structure is wiped out.

5.2. A classical entropy measure

The Kolmogorov–Sinai (KS) entropy, h_{KS}, is a measure of the rate of information production in the system [62]. Thus $h_{\mathrm{KS}} = 0$ only for completely regular dynamics. Pesin [63] showed that KS entropy is equal to the sum of the positive Lyapunov exponents of a chaotic system *i.e.*,

$$h_{\mathrm{KS}} = \sum_{i=1}^{N} \sigma_{(i)}^{+}. \tag{24}$$

The KS entropy (also called dynamical entropy or metric entropy) of a chaotic mapping can be calculated using the formula

$$h_{\mathrm{KS}} = \lim_{t\to\infty} \left(\frac{1}{t}\right) \sum_{n=1}^{t} \log_2 l_n, \tag{25}$$

where

$$l_n = \sqrt{\sum_{a=1}^{d} \left(\delta x_n^{(a)}\right)^2} \tag{26}$$

is the changing distance between two initially close neighbouring points, $(x_0^{(1)}, \ldots, x_0^{(d)})$ and $(x_0^{(1)} + \delta x_0^{(1)}, \ldots, x_0^{(d)} + \delta x_0^{(d)})$, on Σ. $\delta x^{(1)}, \ldots, \delta x^{(d)}$ are evolved by iterating a linearised form of the chaotic map. This *tangent map* is rescaled after every iteration as follows: the n^{th} iteration of the map produces the values $\delta x_n^{(1)}, \ldots, \delta x_n^{(d)}$ from which l_n is calculated. These values are then rescaled to $\delta \bar{x}_n^{(1)} = \delta x_n^{(d)}/l_n, \ldots, \delta \bar{x}_n^{(d)} = \delta x_n^{(d)}/l_n$ which are fed back into the tangent map for the next iteration [54]. Thus l_n is dimensionless. Use of the base-2 logarithm in Eq. (25) allows the entropy to be measured in *bits* of information.

The generalised iterative map $x_{n+1} = f(x_n)$ can be linearised to give its associated d-dimensional tangent map

$$\delta x_{n+1} = f(x_n + \delta x_n) - f(x_n) = g\delta x_n \tag{27}$$

where $g = (g^{(1)}, \ldots, g^{(d)})$. This can be employed in Eq. (25) to calculate h_{KS}.

If $g = g(x_n)$ then the value of h_{KS} will clearly depend on the initial position $(x_0^{(1)}, \ldots, x_0^{(d)})$ on the coordinate space Σ. This is often *not* the case. h_{KS} is generally used as a *global* measure of the level of chaos in a given system, but this is only valuable if all chaotic trajectories in the system can reach into all regions of its coordinate space. Well known examples of such systems include the cat and baker's maps [64].

However for lower values of the chaos parameter K, maps such as the standard map and kicked top map, have a predominantly *mixed* Σ in which different chaotic regions are not connected. g is a function of x_n and invariant rotational tori act as boundaries so that trajectories originating in one chaotic region cannot escape to another. This isolation inhibits the exponential divergence of chaotic trajectories so that h_{KS} will vary from region to region. Thus Eq. (25) becomes a measure of *localised* KS entropy, $h_{\mathrm{KS}}(x_0)$.

To reveal a *complete* description of these maps at a specific K in terms of KS entropy, *many* values of h_{KS} corresponding to many initial positions on Σ can be plotted as a contour map on Σ. Using (25) and (27), and letting $t \to \infty$, values for h_{KS} can be calculated for each point on a large grid of points spanning Σ. Setting $t = 10^5$ iterations, figure 2 shows the KS entropy contour map for the standard map with three different K values.

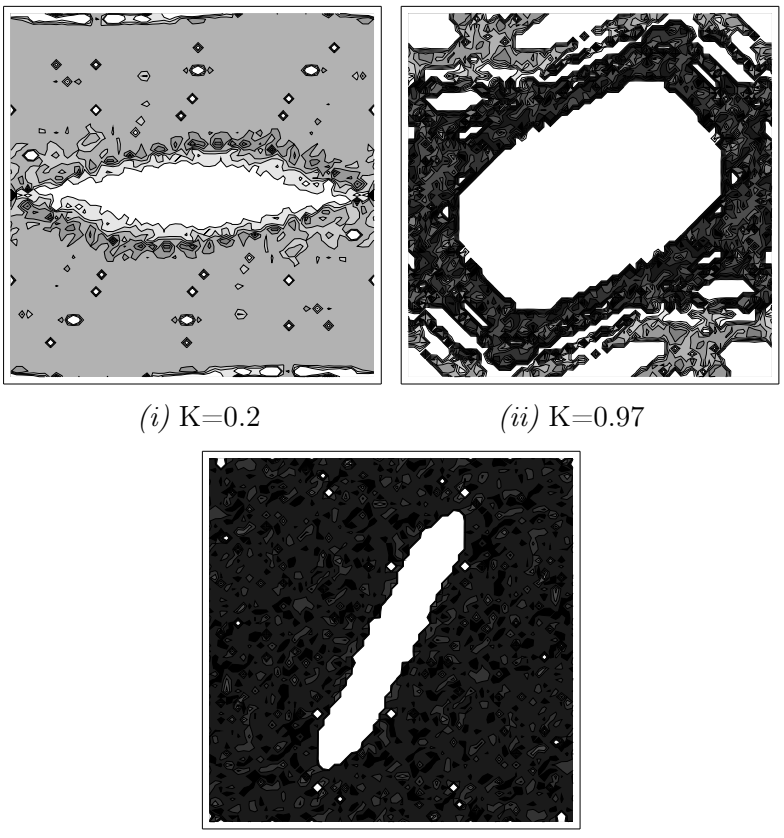

(i) K=0.2 *(ii)* K=0.97

(iii) K=4.0

Fig. 2. KS entropy contour maps for the standard map in unit phase space.

The values for h_{KS} were calculated for each point on a 64×64 grid spanning the same unit of phase space and the same K values as in figure 1(b),(d) and (f). Shading intensity reflects the relative sizes of the KS entropy. $h_{\mathrm{KS}} = 0$ is shown as white on the maps while darker and darker shades of grey reflect an increasing h_{KS}. The black areas show the largest h_{KS} values corresponding to the most chaotic regions of the standard map. The resemblance between figure 1 and figure 2 is striking. Stable islands in the classical maps translate to stark white patches in the contour maps. This is because $h_{\mathrm{KS}} = 0$ for *all* periods in non-chaotic dynamics. The chaotic sea of trajectories in the phase space map are also faithfully reproduced as very dark patches of similar shape and size in the contour map. All these correlations indicate that h_{KS} presented in this way can comprehensively display all the essential features of the standard map as it becomes globally chaotic.

6. Entropy and chaos in quantum mechanics

6.1. Suppression of chaos

It is clear from the last section that the study of classical chaos is a mature and well understood discipline. On the other hand, the very existence of quantum chaos has been plagued with controversy [44, 46, 47]. Classical chaos refers to the dynamical behaviour as $t \to \infty$. It has a fundamentally asymptotic character. We have seen how chaos in classical Hamiltonian dynamics arises because of unstable orbits which cause errors in the initial data to grow exponentially. The situation seems to be very different in quantum mechanics. Here the dynamical law is a unitary evolution of an initial state $\psi_a(0)$:

$$\psi_a(t) = \hat{U}\psi_a(0). \tag{28}$$

Similarly, starting from a slightly different initial state $\psi_b(0)$ yields $\psi_b(t) = \hat{U}\psi_b(0)$ with the same unitary operator $\hat{U}$. It follows that the scalar product of the states ψ_a and ψ_b is constant,

$$\langle \psi_a(t), \psi_b(t) \rangle = \langle \psi_a(0), \psi_b(0) \rangle, \tag{29}$$

so that small imperfections in the preparation of the initial state do not grow. Accordingly, the classical notion of exponentially increasing distance between initially nearby trajectories cannot be translated into quantum theory and so this naive attempt to describe quantum chaos fails.

It has been suggested [72] that the linear nature of the time-dependent Schrödinger equation could be preventing the observation of chaos in quantum mechanics. A classical Hamiltonian system has, however, in addition to

its description in terms of trajectories governed by Hamilton's equations of motion, an equivalent description in terms of Liouville probability densities governed by the Liouville equation. If the time-shift classical operator $\hat{U}$, determined from Hamilton's equations, is defined by

$$(q_t, p_t) = \hat{U}(q_0, p_0) \tag{30}$$

then Liouville's equation represents the conservation of an arbitrary phase volume Γ under the operator $\hat{U}$, *i.e.* [73]

$$\Gamma_t = \hat{U}\Gamma_0 = \Gamma_0. \tag{31}$$

Because it conserves phase space volumes, the linear Liouville equation shares with the Schrödinger equation a lack of sensitivity to initial conditions though it does preserve the chaos of the trajectories [74]. So the argument that the linearity of the Schrödinger equation is responsible for the absence of chaos in quantum mechanics is fallacious.

In fact the correct analogue of a quantum state vector is not a *point* in classical phase space, but a Liouville probability *density*, ρ [75]. This sets the stage for a straightforward generalisation to quantum mechanics.

6.2. Statistical mechanics perspective

The exact point a system occupies in phase space is not generally known in statistical mechanics. The predictions of classical statistical mechanics are derived from a Liouville probability density $\rho(p, q)$ on phase space, which describes incomplete knowledge of the system's phase space position (p, q) and which is the mathematical representation of a system state. The entropy of a system state $\rho(p, q)$, known as the Gibbs entropy or fine-grained entropy, is defined as

$$h_{\mathrm{G}} = -\int d\Gamma(p, q)\rho(p, q)\log_2(\rho(p, q)), \tag{32}$$

where the base-2 logarithm means that the entropy is measured in bits of information. The fact that the Gibbs entropy is formally identical to Shannon's statistical measure of information (*i.e.* Shannon entropy) means that h_{G} can be interpreted as the amount of information missing for a complete specification of the system. Since an infinite amount of information would be needed to give the exact location of a point in phase space, h_{G} is defined up to an arbitrary additive constant.

In quantum mechanics, states described by ρ can be represented either by a Hilbert space vector $|\psi\rangle$ or, more generally, by a density operator $\hat{\rho}$, depending on the preparation procedure. The quantum parallel for Eq. (32), known as the von Neumann (vN) entropy, is defined as

$$h_{\mathrm{vN}} = -\mathrm{Tr}(\hat{\rho}\log_2\hat{\rho}), \tag{33}$$

and measures the information missing toward a complete specification of the quantum system. Since no information beyond that contained in the wave function exists about a quantum system, $h_{\mathrm{vN}} = 0$ for a pure state $\hat{\rho} = |\psi\rangle\langle\psi|$. As a consequence of Eq. (31), both h_{G} and h_{vN} remain constant under Hamiltonian time evolution. Thus no information about the initial state of the system is lost.

To make the connection with thermodynamics, we assume that there is a heat reservoir at temperature T_0, to which all energy in the form of heat must eventually be transferred. In the presence of this reservoir, the free energy *i.e.* the maximum average extractable work, for an equilibrium state is given by

$$F = E - T_0 k_{\mathrm{B}} h \ln 2, \tag{34}$$

where E is the mean internal energy of the state, k_{B} is Boltzman's constant, and $h = h_{\mathrm{G}}$ classically and $h = h_{\mathrm{vN}}$ quantum mechanically. The extractable work is given by Eq. (34) for *any state* of the system, even outside equilibrium [76]. This means that each bit of missing information "costs" $T_0 k_{\mathrm{B}} \ln 2$ of extractable work.

Since entropy is a measure of the state of knowledge about the system, the only way that F can *change* (except for changes in the energy levels) is via a change in the state of knowledge. However, Hamiltonian time evolution of an *isolated* system does not lead to a change in the state of knowledge so entropy and extractable work remain unchanged. As we have seen, this is a consequence of Liouville's theorem and is equally true for regular as for chaotic systems. They are thus indistinguishable since neither gives rise to an information loss.

6.3. Open systems

To use entropy for distinguishing chaotic from regular systems we need a method for the information about the system to change. This is possible in three ways:

6.3.1. Measurement

Extractable work can *increase* if a measurement is made on the system. The accompanying decrease in entropy does not constitute a violation of the sceond law of thermodynamics, however, because the physical state of the observer changes in the course of the measurement. A simple quantitative description of the change in the state of the observer was given by Landauer

[77]. If the observer who performs the measurement wants to use additional information about the system to increase the extractable work, they must keep a physical record of the acquired information. According to Landauer's principle, the erasure of a bit of acquired information in the presence of a T_0 temperature reservoir is *necessarily* accompanied by a dissipation in energy of at least $T_0 k_{\mathrm{B}} \ln 2$. If this thermodynamic cost of erasing acquired information is taken into account as a negative contribution to F, then, on average, no measurement can increase the overall extractable work [78] because it is determined by the sum of entropy *and* acquired information.

6.3.2. Discarding information

Extractable work can *decrease* if information about the system is lost, *i.e.* entropy increases. One mechanism for information loss is by deliberately discarding information and was used by Jaynes [79] to derive traditional thermodynamics. Jaynes showed how equilibrium thermodynamics follows naturally from Liouville's equation if only information about the values of the macroscopic variables defining a thermodynamic state is retained. Unrequired information is discarded by means of the principle of maximum entropy. Coarse graining is another way of discarding unrequired information in which all details below a certain scale are ignored.

6.3.3. Interaction with an incompletely known environment

The second main mechanism for information loss involves the interaction with an incompletely known environment. This leads to a perturbed time evolution of the system. Predictions for the system can then be made by tracing out the environment, *i.e.*, by averaging over the perturbations, which is generally accompanied by an entropy increase.

These three methods all show that a system must be *open* if its evolution is to cause an entropy increase.

7. Quantum entropy measures

To study quantum chaos we need a *quantum* entropy measure that could be employed in a similar way to the classical KS entropy(-rate) discussed earlier. The obvious choice is the rate of von Neumann entropy production. This is a quantitative measure of disorder in quantum statistical mechanics and can also be measured in bits per unit time. As described earlier, the interaction of a system with an incompletely known environment will cause an entropy increase, and thus we first need a way to determine Δh_{vN} for an open quantum system.

7.1. Introducing an environment

Consider a quantum system $\mathcal{S}$ with Hamiltonian

$$\hat{H}_{\mathcal{S}}(\hat{p},\hat{q},t) = \frac{\hat{p}^2}{2} + TKV(\hat{q}) \sum_{n=-\infty}^{\infty} \delta(t-nT). \tag{35}$$

This is a generalisation of the classical Hamiltonian in Eq. (21). Similarly, initial states $|\psi(0)\rangle$ are assumed to be *coherent states*. These can be characterised as minimum-uncertainty states [80] allowing for a close comparison with the classical dynamics. At time t, the system can be described by the density operator

$$\rho(t) = |\psi(t)\rangle\langle\psi(t)| \tag{36}$$

which evolves according to the equation

$$\rho(t+T) = \hat{U}_{\mathcal{S}}\rho(t)\hat{U}_{\mathcal{S}}^{-1}. \tag{37}$$

Here $\hat{U}_{\mathcal{S}}$ is the evolution operator for the system given by

$$\hat{U}_{\mathcal{S}} = \exp\left(\frac{-i\hat{p}^2T}{2\hbar}\right)\exp\left(\frac{-iTKV(\hat{q})}{\hbar}\right). \tag{38}$$

In an experimental situation, the free particle motion would *need* to be periodically opened up to an environment to allow the δ-function "kick" to be introduced. Though Eq. (38) defines the evolution operator for free motion experiencing an *instantaneous* periodic kick, it is equally valid (as long as the free motion is not concurrent [59]) for a *finite* time periodic kick which is what is required to perform this experimentally. Requiring a quantum system to be open to achieve an entropy increase is thus not just a convenient mathematical construction but a necessary condition for an experimental realisation.

We choose, therefore, the environmental coupling to mirror the form of the kick in Eq. (35) with regard to the $\hat{q}$ dependence and interaction time. We also choose the environmental model to be a collection of degenerate two-state systems with a range of interaction strengths governed by a normal distribution. This is a generalisation of the class of environments considered by Schack and Caves [51]. Thus we have an interaction Hamiltonian

$$\hat{H}_{\mathcal{I}} = \varepsilon V(\hat{q}) \otimes \sum_{n=-\infty}^{\infty} \hat{\sigma}_z(n)\delta(t-nT). \tag{39}$$

During the nth kick $\mathcal{S}$ interacts with a single two state system $\mathcal{I}$. This has Pauli operator $\hat{\sigma}_z(n)$ and interaction strength ε. Each of the two-state

enviroment systems is equally likely to in the "up" state $|\uparrow\rangle$, where $\hat{\sigma}_z|\uparrow\rangle = |\uparrow\rangle$, or in the "down" state $|\downarrow\rangle$, where $\hat{\sigma}_z|\downarrow\rangle$. During each kick the distribution P_ε for ε is the normal distribution $N(\varepsilon_0, \varepsilon_{\rm var})$.

The combined (total) Hamiltonian for the coupled system and environment is thus

$$\hat{H}_{\mathcal{T}} = \hat{H}_{\mathcal{S}} + \hat{H}_{\mathcal{I}} \tag{40}$$

and the corresponding density operator evolution equation is

$$\rho(t+T) = \hat{U}_{\mathcal{T}}(\varepsilon,\beta)\ \rho(t)\ \hat{U}_{\mathcal{T}}^{-1}(\varepsilon,\beta)\,. \tag{41}$$

Here $\hat{U}_{\mathcal{T}}$ is the combined evolution operator given by

$$\hat{U}_{\mathcal{T}}(\varepsilon,\beta) = \hat{U}_{\mathcal{I}}\hat{U}_{\mathcal{S}}\,, \tag{42}$$

where

$$\hat{U}_{\mathcal{I}} = \exp\left(\frac{-i\varepsilon\beta T V(\hat{q})}{\hbar}\right)\,. \tag{43}$$

$\beta \in \{-1, 1\}$ and is the result of measuring the two state environment after each interval T to determine whether it is an up or down state. As before, this same operator would result if Eq. (39) was turned on for the *finite* time required for an experimental realisation of this system.

The effect of this environmental coupling is to produce a multiple stochastic perturbation at the end of each time interval. Roughly speaking, Eq. (43) acts like a momentum shift operator, the extent of the shift being dependent on ε at every time step. If ε_p is the magnitude of the momentum shift measured in units of the separation between momentum eigenstates then

$$\varepsilon_p = \frac{\varepsilon}{2\pi\hbar}\,. \tag{44}$$

We can model $N(\varepsilon_0, \varepsilon_{\rm var})$ with a symmetric binomial distribution such that ε is drawn from a large collection of $R+1$ independent interaction strengths. Thus after each interval, there are $2R+2$ different measurement results leading to $2R+2$ possible pure states for the system. Averaging over all these possible outcomes in the position basis produces the density operator evolution equation for $\mathcal{S}$ which is

$$\begin{aligned}
\bar{\rho}_{ab}(t+T) &\equiv \langle a|\ \bar{\rho}(t+T)\ |b\rangle \\
&= \sum_{r=1}^{R+1} \frac{P_{\varepsilon_r}}{2} \sum_{\beta=-1,1} \langle a|\ \hat{U}_{\mathcal{T}}(\varepsilon_r,\beta)\ \bar{\rho}(t)\ \hat{U}_{\mathcal{T}}^{-1}(\varepsilon_r,\beta)|b\rangle \\
&= F(a,b)\ \langle a|\ \hat{U}_{\mathcal{S}}\ \bar{\rho}(t)\ \hat{U}_{\mathcal{S}}^{-1}\ |b\rangle\,,
\end{aligned} \tag{45}$$

where

$$F(a,b) = \sum_{r=1}^{R+1} P_{\varepsilon_r} \cos\left(\frac{\varepsilon_r[V(a)-V(b)]}{\hbar}\right) \tag{46}$$

now contains all the perturbation effects due to the environment. This results in a vN entropy increase, $\Delta h_{\rm vN}$, which can be determined by

$$\Delta h_{\rm vN}(nT) = -{\rm Tr}(\bar{\rho}(nT)\log_2\bar{\rho}(nT))\,, \tag{47}$$

where $\bar{\rho}(nT)$ is the average density matrix of the system after n time steps.

We are now in a position to calculate the von Neumann entropy production rate, $\tilde{h}_{\rm vN}$. Setting $T=1$, this can be approximated in discrete time by

$$\tilde{h}_{\rm vN} \approx \Delta h_{\rm vN}(n) - \Delta h_{\rm vN}(n-1)\,. \tag{48}$$

Using this and expanding the cosine in Eq. (46) and the logarithm in Eq. (47) as power series, the rate of vN entropy production in a D-dimensional Hilbert space can be written explicitly:

$$\begin{aligned}\tilde{h}_{\rm vN} \;\approx\; & \sum_{m=1}^{\infty}\sum_{q=1}^{m}\binom{m}{q}\frac{(-1)^{q+1}}{m\ln 2}\sum_{a_1\ldots a_{q+1}}^{D}\left(\sum_{l=1}^{q+1} f(a_l,a_{l+1})\right)\\ & \times\prod_{l'=1}^{q+1}\langle a_{l'}|\hat{U}_{\mathcal{S}}\bar{\rho}(n-1)\hat{U}_{\mathcal{S}}^{-1}|a_{l'+1}\rangle\,,\end{aligned} \tag{49}$$

where $D=(2\pi\hbar)^{-1}$, l is cyclic ($l_{q+2}=l_1$) and

$$f(a_l,a_{l+1}) = \sum_{r=1}^{R+1} P_{\varepsilon_r}\sum_{j=1}^{\infty}\frac{(-1)^{j+1}}{(2j)!}\left(\frac{\varepsilon_r[V(a_l)-V(a_{l+1})]}{\hbar}\right)^{2j}. \tag{50}$$

It should be noted that the total entropy increase is bounded by a maximum,

$$(h_{\rm vN})_{\max} = -\sum_{j=1}^{D}\left(\frac{1}{D}\right)\log_2\left(\frac{1}{D}\right) = \log_2 D\,. \tag{51}$$

This is only attained when the density matrix is a completely random ensemble [81]. Clearly, $(h_{\rm vN})_{\max}$ is limited by the dimensions of the Hilbert space.

7.2. Linear entropy

Linear entropy [82] is a measure of the purity of a state. It is defined as

$$h^{\text{lin.}} = \text{Tr}(\rho - \rho^2). \tag{52}$$

and has been used to reveal the selection of the preferred classical set of states in the process of quantum decoherence [83].

Keeping only the first term ($m = 1$) in the logarithm expansion in Eq. (49) yields the linear entropy production rate:

$$\tilde{h}_{\text{vN}}^{\text{lin.}} \approx \sum_{a_1,a_2}^{D} (f(a_1,a_2) + f(a_2,a_1)) \left|\langle a_1|\hat{U}_{\mathcal{S}}\bar{\rho}(n-1)\hat{U}_{\mathcal{S}}|a_2\rangle\right|^2. \tag{53}$$

Assuming $\varepsilon_{\text{var}} \ll 1$ we only need to keep the first term of the j expansion in Eq. (50). Thus

$$f(a_1,a_2) = \sum_{r=1}^{R+1} \frac{P_{\varepsilon_r}\varepsilon_r^2}{2} \left(\frac{[V(a_1) - V(a_2)]}{\hbar}\right)^2. \tag{54}$$

However,

$$\sum_{r=1}^{R+1} P_{\varepsilon_r}\varepsilon_r^2 = \varepsilon_{\text{var}}, \tag{55}$$

so that

$$\tilde{h}_{\text{vN}}^{\text{lin.}} \approx \frac{\varepsilon_{\text{var}}}{\ln 2} \sum_{a_1,a_2}^{D} \left(\frac{[V(a_1) - V(a_2)]}{\hbar}\right)^2 \left|\langle a_1|\hat{U}_{\mathcal{S}}\bar{\rho}(n-1)\hat{U}_{\mathcal{S}}|a_2\rangle\right|^2. \tag{56}$$

This gives us an idea of the parameter dependence of $\tilde{h}_{\text{vN}}$. At each timestep the linear entropy production rate is proportional to the variance of the distribution of interaction strengths as well as being dependent on the specific nature of the environment. Thus the strength and nature of the environment are expected to effect the rate of entropy increase. This is intuitively satisfying since the ultimate source of quantum entropy production is the environmental coupling.

8. Quantum-classical correspondence

As we stated earlier Zurek and Paz [52, 53] have conjectured that for an *open* quantum system with minimal dissipation which displays classical chaos, the *rate* of vN entropy production, $\tilde{h}_{\text{vN}}$, of its quantum analogue,

after an initial decoherence time, $t_{\rm d}$, will rise to a maximum value which is equal to the sum of its positive Lyapunov exponents. This "entropy rate plateau" will be sustained until the system begins to approach equilibrium when $\tilde{h}_{\rm vN}$ will slowly decrease. It will reach zero at a time $t_{\rm eqm}$ when the entropy increases to a maximum as in Eq. (51). In contrast, for the quantum analogue of a regular system, the entropy production rate will asymptotically tend to zero well before $t_{\rm eqm}$. These possibilities are shown in figure 3.

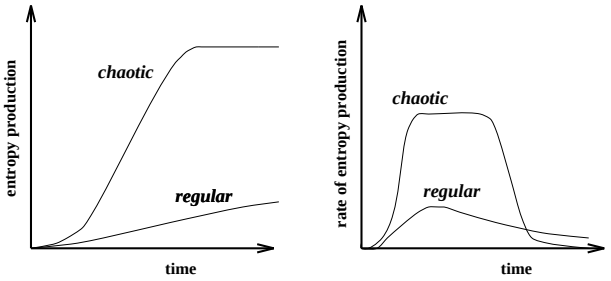

Fig. 3. The correspondence conjecture.

8.1. Theory

Since $h_{\rm KS}$ is equal to the sum of the positive Lyapunov exponents of a classically chaotic system (Eq. (24)), this correspondence conjecture can be written as

$$\tilde{h}_{\rm vN} = h_{\rm KS}. \tag{57}$$

With reference to the above system $\mathcal{S}$ interacting with an environment, the Zurek and Paz conjecture implies that the discrete time $\tilde{h}_{\rm vN}$ should be approximately equal to the KS entropy of its unperturbed counterpart in classical mechanics. Thus if

$$t_{\rm d} < n \ll t_{\rm eqm}, \tag{58}$$

then

$$\tilde{h}_{\rm vN} \approx \Delta h_{\rm vN}(n) - \Delta h_{\rm vN}(n-1) \approx h_{\rm KS}. \tag{59}$$

The onset of decoherence at time $t_{\rm d}$ is essentially independent of $\hat{H}_{\mathcal{S}}$, but is dependent on the strength and nature of the coupling with the environment described by $\hat{H}_{\mathcal{I}}$ and on the form of the initial state.

Suprisingly however, the conjecture of Zurek and Paz expects that for a system weakly coupled to an environment and fulfilling Eq. (58), the nature

and strength of the environmental coupling will *not* effect the correspondence described in Eq. (57) [84]. Our derivations of the discrete time $\tilde{h}_{\rm vN}$ in Eq. (49), and $\tilde{h}^{\rm lin.}_{\rm vN}$ in Eq. (56), clearly show that the environment *will* effect the correspondence relation.

We will numerically calculate vN entropy production rates for two quantum systems with a range of environmental coupling strengths. This will lead to a *modified* version of the correspondence conjecture advocated by Zurek and Paz. Also, since we now have a formal way of calculating quantum entropy production rates, we can produce vN entropy production rate contour maps and their associated multifractal spectra.

8.2. Shadowing

There is an immediate challenge to the correspondence conjecture as a result of introducing an environment. The Hamiltonian of the *coupled* system described in Eq. (40) no longer corresponds to the classical one. By comparing Eq. (38) with Eq. (43), it is clear that K will be replaced by $K + \varepsilon\Lambda$ in the map derived from the classical limit of the coupled quantum Hamiltonian. This mapping is like the generic classical map but with a small perturbation (whose strength and sign is randomly chosen at each time step) added to the chaos parameter K.

By rewriting this mapping as

$$\begin{aligned} q_{n+1} &= q_n + p_{n+1} \\ p_{n+1} &= p_n + \delta_n - K\left(\frac{\partial V}{\partial q}\right)_{q=q_n}, \end{aligned} \tag{60}$$

where

$$\delta_n = (\varepsilon\beta)_n \left(\frac{\partial V}{\partial q}\right)_{q=q_n}, \tag{61}$$

we can now view the classical perturbation as a small random displacement in phase space at every time step. This noisy classical mapping is comparable to the noise generated by round-off errors in the numerical computation of classical chaotic trajectories. Once again we can invoke the shadowing property to argue that the noisy classical map in Eq. (60) will generate the same localised KS entropy measures as the generic classical map provided that the noise level is below a certain bound.

8.3. Results for the standard map

Quantum entropy measures for the standard map [91] can be found by following the theory in Section 7.1 while setting $V(q) = \cos(4\pi\hat{q})/4\pi^2$. A uniformly spaced 64×64 grid of initial coherent states (corresponding to an

even spread over unit phase space) were numerically evolved in time. Using Eq. (48), the maximum value of $\tilde{h}_{vN}$ for each evolution was plotted on a contour map in a similar fashion to the classical case. Figure 4 displays the results for three values of K with $D = 256$, $\varepsilon_0 = 0.001$, $\varepsilon_{\text{var}} = 0.2\varepsilon_0$, $R = 100$ and $T = 1$.

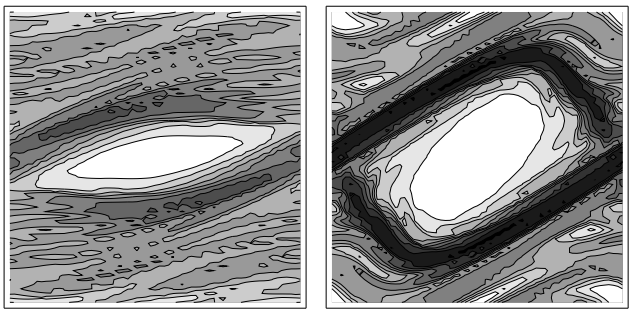

(i) K=0.2 *(ii)* K=0.97

(iii) K=4.0

Fig. 4. Contour plots of the vN entropy production rate in unit phase space for the quantum kicked rotor (standard map) interacting with an environment

There are remarkable similarities between figure 2 and figure 4. For the same K values, the size and location of the various stable islands is analogous, dark patches are prevelant in the heavily chaotic regions, the axes of symmetry are consistent and the overall complexity of the dynamics is clearly visible in both.

There are also differences. The quantum contour maps are generally much smoother than their classical counterparts. This is because each initial coherent state in the quantum system has a support area causing their evolution to imitate that of a *density* of points on phase space. Thus neighbouring coherent states will fail to achieve dramatically different rates of vN entropy production. Increasing D reduces the supports of the initial

coherent states as well as reducing the overlap between neighbouring states. It was found that this led to a reduction in the smoothness of the quantum contour maps making them more greatly resemble the classical contour maps.

The process of calculating these entropy contour maps was repeated with variations to $N(\varepsilon_0, \varepsilon_{\text{var}})$. For $\varepsilon_0, \varepsilon_{\text{var}} \ll K$, when any entropy increase is due primarily to the chaotic dynamics of the system and not the interaction, similar results were achieved.

9. Generalised cat map investigations

To investigate further the notions of classical chaos and the corresponding quantum chaos discussed in previous sections we now turn to a simple one dimensional system — the generalised cat map. We review the classical dynamics of this map, show its chaotic nature based on established definitions and highlight some special features which will be useful when looking at its quantised counterpart. We make entropy comparisons between the classical and quantum generalised cat systems based on the theory of the previous sections and present a mathematical relationship between these entropies.

9.1. The classical map

Even though the generalised cat map is much simpler than the standard map previously discussed it has a number of peculiar qualities that make it worthy of investigation. Firstly, it is a straightforward piecewise *linear* system capable of chaotic motion. Secondly, it displays an abrupt transition between dynamical regimes by never having a mixed phase space. The map can thus only be globally regular or globally chaotic. Thirdly, being a well known system [47, 64, 85–89] its ability to act chaotically in the quantum regime is of general interest.

9.1.1. Phase space dynamics

Introducing a simple nonlinear potential energy function $V(q) = -Kq^2/2\sum_{n=-\infty}^{\infty}\delta(t-n)$ to replace the potential in Eq. (21) and imposing periodic boundary conditions in both q and p gives rise to the mapping

$$\begin{aligned} p_{n+1} &= p_n + Kq_n \pmod{p=1}, \\ q_{n+1} &= q_n + p_{n+1} \pmod{q=1}. \end{aligned} \tag{62}$$

Here K is a real variable which acts as the chaos parameter and the dynamics of the system is confined to the unit phase space torus.

The positive integer values of K produce a class of maps known as the *cat maps* [64]. The name comes from the fact that their chaotic nature is traditionally illustrated by showing the result of their evolution on the face of a cat. The class of maps for noninteger K are known as the *sawtooth maps* [85]. This name comes from the graph of the 'kick term' in Eq. (62) *versus* position *i.e.* plotting $Kq \ (\mathrm{mod} q = 1)$ against q produces a repeated sawtooth shape. Though the cat and sawtooth maps have some distinguishing features (*e.g.* the cat map can be obtained from a non-periodic but the sawtooth map cannot), we treat them as part of a family of mappings because simply varying K in Eq. (62) can produce both. We choose the *generalised cat map* (GCM) as their collective name.

The GCM is already linear so, following Eq. (27), its associate tangent map is simply

$$\begin{pmatrix} \delta p_{n+1} \\ \delta q_{n+1} \end{pmatrix} = \begin{pmatrix} 1 & K \\ 1 & 1+K \end{pmatrix} \begin{pmatrix} \delta p_n \\ \delta q_n \end{pmatrix}. \tag{63}$$

and is independent of phase space position for all times. The two eigenvalues, $\Lambda_\pm$, of this map are $x \pm \sqrt{x^2-1}$, where $x = 1 + K/2$. The dynamics of the GCM thus fall into two K dependent categories:

(i) When $K > 0$ or $K < -4$ then $\Lambda_+ > 0 > \Lambda_-$. In this case *all* points in the phase space are hyperbolic (saddle points) so that the distance between neighbouring trajectories exponentially expands in one direction while exponentially contracting in another. The map is thus chaotic for *all* initial conditions.

(ii) When $-4 \leq K \leq 0$ then

$$\Lambda_\pm = x + iy = e^{\pm i\theta}, \tag{64}$$

where $x = \cos\theta$ and $y = \sin\theta = \sqrt{1-x^2}$. In this case there are both periodic and quasiperiodic phase space orbits densely spread throughout the K value range. The smallest periodic orbit, P, is 4 for $K = -2$. Moving away from this value in both directions, all possible periodic orbits can be identified until $P \to \infty$ as $K \to -4$ and $K \to 0$. When $K = 0$ the dynamics are just those of a free rotor. No phase space points evolve exponentially so the map is everywhere regular.

Figure 5 shows the phase space of the GCM for a number of K values. Each one is the result of iterating several initial points 10^5 times. For (b) to (e) the map is globally regular, having a central elliptic island surrounded by an intricate set of other smaller islands which fill up the phase space. As K is increased the extent of stretching and folding of the islands is reduced. Specifically, the large central island no longer encounters folding when $K \geq 1$. In (a) and (f) the map is globally chaotic so that there is no phase space structure at all.

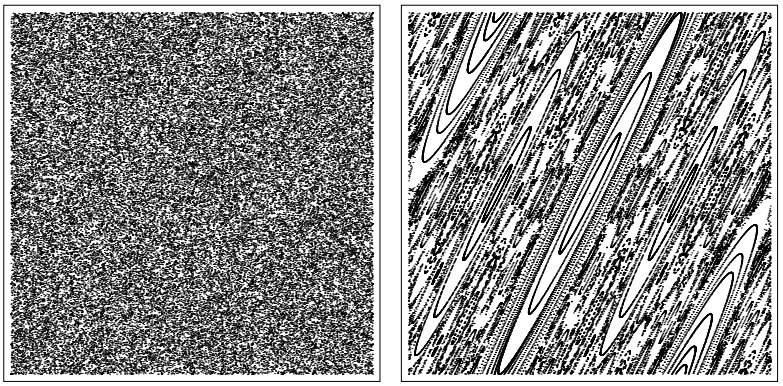

(a) $K = -5.0$ (b) $K = -3.9$

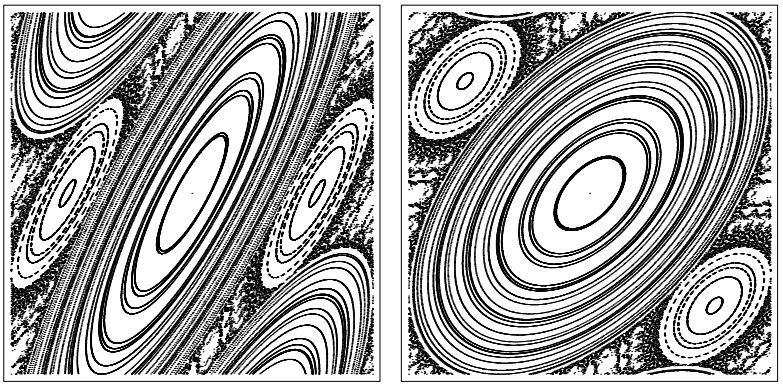

(c) $K = -2.9$ (d) $K = -1.1$

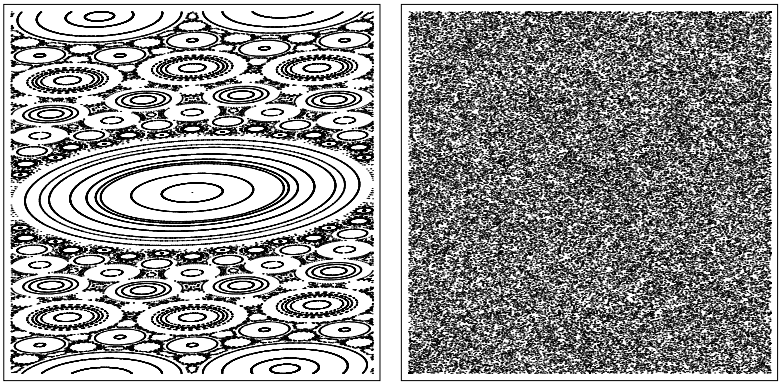

(e) K=–0.1 (f) K=1.0

Fig. 5. Phase space of the varying K values bounded on the interval $[-\frac{1}{2}, \frac{1}{2})$ for both q and p.

9.1.2. KS entropy measures

The two Lyapunov exponents of the GCM are $\sigma_{\pm} = \ln(x \pm \sqrt{x^2 - 1})$. Also, using Eq. (24), the KS entropy of the map, in bits, is

$$h_{\mathrm{KS}} = \log_2(x + \sqrt{x^2 - 1}), \tag{65}$$

and when K is large $h_{\mathrm{KS}} \approx K$. Using Eq. (63) in (25), with

$$l_n = \sqrt{(\delta p_n)^2 + (\delta q_n)^2}, \tag{66}$$

we have calculated the KS entropy as a function of K. This is shown in figure 6 for a large number of K values, with $t = 10^5$. The graph shows the abrupt switch from globally regular to globally chaotic dynamics at $K = -4$ and $K = 0$. It is symmetric about the $K = -2$ axis.

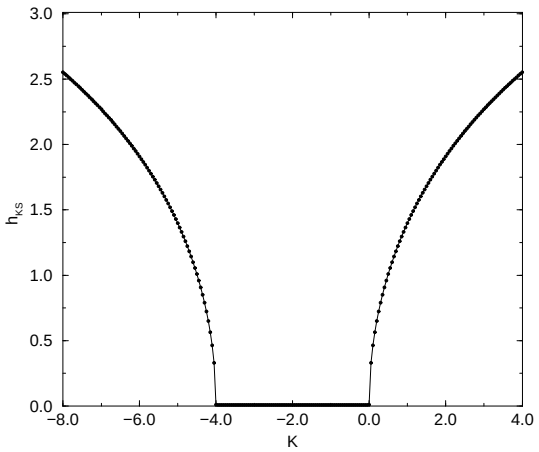

Fig. 6. KS entropy *vs.* K for the GCM.

9.1.3. A divergence measure for regular dynamics

Though the KS entropy gives a measure of the GCM's dynamics in the chaotic regime, it is not very useful in the regular regime because $h_{\mathrm{KS}} = 0$ for all nonchaotic motion. Can we find a measure that will reflect the changing structure in the phase space of the regular GCM described in Fig. 5(b)-(e)?

From Eq. (64) we know that the eigenvalues for the tangent map are complex in the regular regime and, as shown in figure 7, form an argand diagram with radius 1. Like figure 6, this gives the impression that the dynamics of the map are symmetric about $K = -2$.

However, it is clear from the phase space diagrams in figure 5 that the regular dynamics are much more erratic for $-4 < K < 2$ than $-2 < K0$.

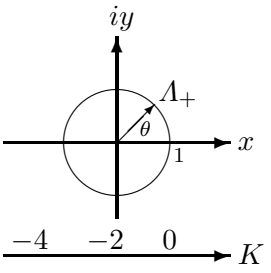

Fig. 7. Argand diagram for eigenvalues of the regular GCM

We need a formula that is sensitive to the changing shapes of the elliptic islands in phase space. The amount of stretching of the elliptic islands in the GCM map depends on Eq. (66). However, for regular dynamics the divergence is *not* exponential — it only grows linearly (or possibly algebraically) — therefore the logarithmic measure described in Eq. (65) is not suitable. Paralleling the well known Lyapunov characteristic exponent definition we therefore suggest the following

$$\sigma_{\rm div} = \lim_{t\to\infty} \lim_{d(0)\to 0} \left(\frac{1}{t^R}\right) \left[\frac{d(t)}{d(0)}\right] , \tag{67}$$

where R is the highest power in the algebraic expression that the describes the nature of the divergence. In the case of the discrete time 1-dimensional GCM, assuming a polynomial divergence growth, we can then define a calculable pseudo-entropy divergence measure

$$h_{\rm div} = \lim_{t\to\infty} \left(\frac{1}{l_0 t^{R+1}}\right) \sum_{n=1}^{t} l_n \,, \tag{68}$$

where the growth rate of l_n is parameterised by the polynomial coefficients c_r so that

$$l_n = \sum_{r=1}^{R} c_r n^r . \tag{69}$$

In this adaptation of Eq. (25) the distance between neighbouring points does not need to be rescaled after every time step because the divergence is not exponential.

If we now assume a linear growth in the divergence of neighbouring phase space points in the GCM then $R = 1$ and Eq. (68) becomes

$$h_{\rm div} = c_1/2l_0 \,, \tag{70}$$

because

$$\sum_{n=1}^{t} n = t(t+1)/2. \tag{71}$$

Setting $t = 10^5$, figure 8 shows the numerical results of plotting h_{div} against K with this assumption. At $K = -4$ and $K = 0$ (shown by vertical dashed lines), the graph gradually approaches infinity as expected. However, in between it produces a very interesting non-symmetric shape. As K decreases, the h_{div} curve quickly drops to a minimum just beyond $K = -1$. The curve then begins to rise at a *slower* rate than the previous decline. The approach to infinity at $K = -4$ thus starts earlier, and is also much slower, than at $K = 0$.

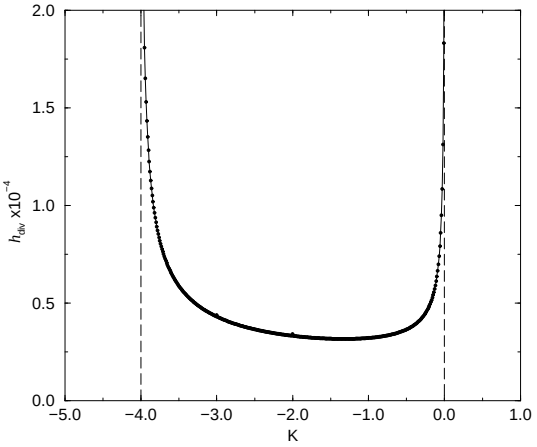

Fig. 8. Divergence plot for the regular GCM

The shape of this curve parallels the amount of stretching and folding of the larger elliptic islands displayed in figure 5(b) to (e). When the curve drops into the regular regime at $K = 0$, there is no folding and little stretching of these islands — see (e) in Fig. 5 — until $K = -1$. Thus h_{div} quickly falls to a minimum. However, for $K \leq -1$, these islands begin to stretch and fold more and more — see (d) to (b) in Fig. 5 — causing h_{div} to gradually increase. Also, comparing the difference in stretching and folding of these islands in (b) and (e) of Fig. 5 explains why h_{div} near $K = -4$ is much larger than near $K = 0$.

In a similar set up with $R = 2$ (and in fact for $R \geq 2$), the numerical results gave $h_{\text{div}} = 0$ for all values of K. This suggests that the assumption of *linear* divergence growth in the case of the regular GCM is reasonable.

We now have a calculable measure of the GCM's regular phase space dynamics. Just as h_{KS} measures the exponential divergence of neighbour-

ing phase space points when the GCM displays chaotic dynamics, so $h_{\rm div}$ measures the linear divergence of neighbouring phase space points when the GCM displays regular dynamics. We thus have a comprehensive method of measuring the nature of the dynamics of the GCM for *all* values of the chaos parameter K.

9.2. The quantum map

We now quantise the generalised cat map and then closely follow the procedure described in Section 7.1 of introducing a suitable perturbing environment. The quantised model of the GCM is governed by the Hamiltonian

$$\hat{H}_{\rm GCM}(\hat{p},\hat{q},t) = \frac{\hat{p}^2}{2} - \frac{K\hat{q}^2}{2}\sum_{n=-\infty}^{\infty}\delta(t-n)\,. \tag{72}$$

Following Refs. [34,80] and [90], the kinematics are that of finite-dimensional quantum mechanics with periodic boundary conditions. Position and momentum space are thus discretised, placing the lattice sites at discrete values

$$q_x, p_x = x/D\,, \tag{73}$$

for $x = -D/2,\ldots,D/2-1$. The dimension D of Hilbert space is taken as even and, for consistency of units, the quantum scale on phase space is taken to be $2\pi\hbar = 1/D$. The periodicised position and momentum basis kets are denoted by $|q_x\rangle$ and $|p_y\rangle$ respectively. The transformation functions are discretised plane waves,

$$\langle q_x|p_y\rangle = \frac{1}{\sqrt{D}}\exp\left(\frac{2\pi i x y}{D}\right)\,. \tag{74}$$

Initial states, $|\psi_0\rangle$, are chosen as follows. We define a family of D^2 states $|q_x,p_y\rangle$, which can be treated as (minimum uncertainty) coherent states in analogy to the continuous case. The fiducial initial coherent state

$$|\psi_{0\{0,0\}}\rangle = |q_0,p_0\rangle \tag{75}$$

is defined as the ground state of a special Harper operator [80] *i.e.* the eigenstate with the smallest eigenvalue of the operator

$$2-\cos(2\pi\hat{q})-\cos(2\pi\hat{p}). \tag{76}$$

This can be displaced with the appropriate operators to identify all the other possible initial coherent states $|\psi_{0\{x,y\}}\rangle = |q_x,p_y\rangle$, *i.e.*,

$$|\psi_{0\{x,y\}}\rangle = \exp\left(\frac{i\pi x y}{D}\right)\exp(-2\pi i x\hat{p})\exp(2\pi i y\hat{q})|\psi_{0\{0,0\}}\rangle. \tag{77}$$

The unitary evolution operator for one step is

$$\hat{U}_{\mathrm{GCM}} = \exp\left(\frac{-i\hat{p}^2}{2\hbar}\right)\exp\left(\frac{iK\hat{q}^2}{2\hbar}\right). \tag{78}$$

Following Section 7.1, we introduce an environmental coupling which mirrors the form of the kick in Eq. (72) with regard to the $\hat{q}$ dependence and interaction time. The interaction Hamiltonian is thus

$$\hat{H}_{\mathrm{interaction}} = \frac{\varepsilon K\hat{q}^2}{2} \otimes \sum_{n=-\infty}^{\infty} \hat{\sigma}_z(n)\delta(t-n). \tag{79}$$

and the combined evolution operator for the quantised perturbed GCM is

$$\hat{U}_{\mathrm{total}}(\varepsilon,\beta) = \exp\left(\frac{i\varepsilon\beta\hat{q}^2}{2\hbar}\right)\hat{U}_{\mathrm{GCM}}. \tag{80}$$

Following Eq. (45), the iterative density evolution operator for the coupled system from timestep $n-1$ to time step n is

$$\bar{\rho}(n+1) = F(a,b)\langle a|\hat{U}_{\mathrm{total}}\hat{\rho}(n)\hat{U}^{-1}_{\mathrm{total}}|b\rangle\,, \tag{81}$$

where

$$F(a,b) = \sum_{r=1}^{R+1} P_{\varepsilon_r}\cos\left(\frac{\pi\varepsilon_r[a^2-b^2]}{D}\right). \tag{82}$$

The rate of von Neumann entropy increase after n time steps can then be calculated using

$$\tilde{h}_{\mathrm{vN}} \approx \Delta h_{\mathrm{vN}}(n) - \Delta h_{\mathrm{vN}}(n-1)\,, \tag{83}$$

where

$$\Delta h_{\mathrm{vN}}(n) = -\mathrm{Tr}(\bar{\rho}(n)\log_2\bar{\rho}(n))\,, \tag{84}$$

and $\bar{\rho}(n)$ is the average density matrix of the system at that time step.

Using Eq. (60), we can write the perturbed GCM associated with the classical limit of the coupled quantum system as

$$\begin{aligned} p_{n+1} &= p_n + K(q_n + \delta q_n), \\ q_{n+1} &= q_n + p_{n+1}\,, \end{aligned} \tag{85}$$

where $\delta q_n = (\varepsilon\beta)_n q_n/K$ and mod $p,q = 1$. The discussion in Section 8.2 about the shadowing property implies that for small perturbations, the maps in Eqs. (62) and (85) should lead to very similar entropy measures.

We used Eq. (85) to calculate h_{KS} and h_{div} for similar K values and for a range of $\varepsilon_{\mathrm{var}}$ which, as in the quantum case, govern the perturbation

strength. We compared these results with the numerical results plotted in figures 6 and 8. When $\varepsilon_{\text{var}} \leq 0.1$ all the h_{KS} results for the perturbed and unperturbed systems matched to at least two decimal places. Due to the nature of Eq. (70), perturbations in K have a much larger impact on h_{div} than h_{KS} so that the h_{div} results for the perturbed and unperturbed systems do not match up very well unless $\varepsilon_{\text{var}} \ll 0.1$. However, the overall *shape* of the unsymmetric curve is common to both.

As expected, for small perturbations ($\varepsilon_{\text{var}} \leq 0.1$), we can assume that the entropy rate measures of the chaotic dynamics of our quantised system are comparable with the equivalent measures for the (unperturbed) classical GCM. For regular dynamics only overall shapes of entropy rates vs. K plots can be reasonably compared.

9.3. vN entropy results

This section contains the results of numerical computations of von Neumann entropy performed on the perturbed quantum map. By varying the parameters described below, a large array of data was produced which can be used to investigate the quantum-classical correspondence of the GCM system described in the previous chapter.

ε_{var} is the variance of the normal distribution of interaction strengths and is a measure of the coupling between the map and the perturbing environment.

D is the dimension of the Hilbert space.

K is a measure of the extent of dynamical chaos in the GCM.

$|\psi_{0\{x,y\}}\rangle$ describes the initial state of the system.

In our computations the normal distribution is modelled by a binomial distribution of $R+1$ terms and mean ε_0. We set $R = 100$ and $\varepsilon_0 = 0$ for all the results.

The plateau heights were computed in the same way for every result: The von Neumann entropy rate was calculated for the first ten steps of the discrete time evolution n. This was long enough to contain the complete plateau. Then the three largest values of $\tilde{h}_{\text{vN}}$ were averaged to give the average height of the entropy rate plateau.

Starting with the fiducial initial state $|\psi_{0\{0,0\}}\rangle$ the coupled GCM quantum system was numerically evolved in discrete time using Eq. (81). Then using Eq. (83), entropy rate plateaux were calculated for a range of chaos parameters K and a range of environmentally-induced perturbation strengths governed by ε_{var}. The results, for $D = 256$ and $D = 512$, are displayed in

figures 9 and 10. The vertical dashed lines mark out the two transitions to global chaos in the corresponding classical dynamics and are shown to aid the discussion of quantum-classical correspondence.

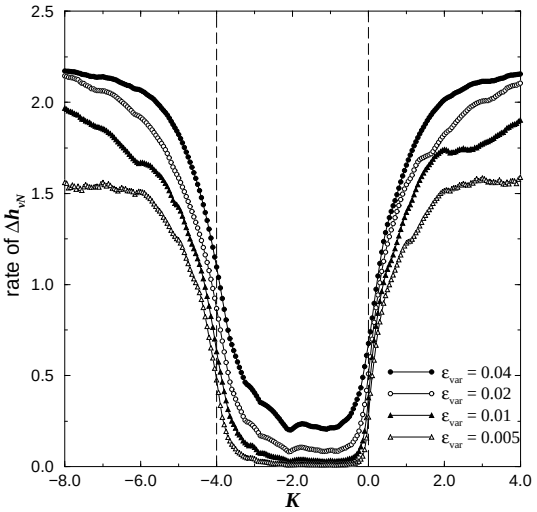

Fig. 9. Quantum GCM: Entropy rate plateaux for a range of K with $D = 256$.

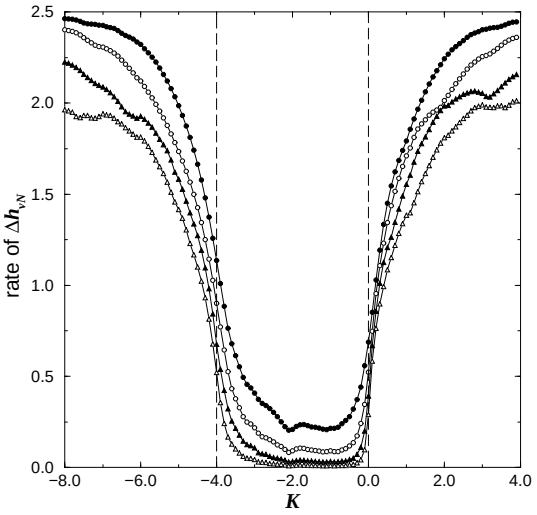

Fig. 10. Quantum GCM: Entropy rate plateaux for a range of K with $D = 512$ (key is the same as above).

The overall *shapes* of the curves in figures 9 and 10 are remarkably similar to the classical case of figure 6 in that the chaotic and regular regions are

clearly distinct and there is a rough symmetry about $K = -2$. There are however a number of differences in each of the two regions:

9.3.1. The chaotic region

Unlike the classical case, the entropy rate plateaux in figures 9 and 10 begin to level off for increasing $|K|$. There are two separate reasons for this depending on the size of ε_{var} which is used.

When ε_{var} is small (*e.g.* the $\varepsilon_{\text{var}} = 0.005$ curve in both figures), the perturbation strength is not large enough to cause complete decoherence. Unlike the anharmonic oscillator discussed by Zurek and Paz in the correspondence conjecture, the GCM exhibits *folding* as well as stretching. Increasing $|K|$ produces more folding and a faster development of fine structure in the classical phase space patch. Due to interference effects, this cannot be imitated in the quantum GCM.

When ε_{var} is large (*e.g.* the $\varepsilon_{\text{var}} = 0.04$ curve in both figure), saturation problems come into play. The combined effect of a large perturbation strength and an increasing $|K|$ cause the vN entropy to quickly approach its maximum value. $(h_{\text{vN}})_{\max} = 8$ for figure 9 and 9 for 10). Thus the increase of the vN entropy production *rate* will then be curtailed and the entropy rate plateau will not faithfully reflect the peak rate.

9.3.2. The regular region

The discontinuity in the transitions from chaotic to regular dynamics in the classical system become smooth gradual transitions in its quantum counterpart. Also, though the (KS) entropy rate falls to zero in the regular regions of the classical system, in the quantum system these regions contain finite (vN) entropy rates which increase with ε_{var}.

These differences are a result of the influence of the perturbing environment as well as the *nature* of the vN entropy measure. The fact that the environment is itself a source of entropy increase means that even in the regular regions we do not expect the quantum entropy rate curves to fall to zero. In these regions, we would expect $\tilde{h}_{\text{vN}}$ to be held constant, with values proportional to ε_{var}. However, the pronounced structure of the curves in figures 9 and 10 implies that the quantum system is sensitive to the varying K.

In Section 9.1.3 we described a pseudo-entropy divergence measure, h_{div}, that is sensitive to varying K for the *classical* regular GCM. Away from the transition points ($K = 0, 4$) the shape of the h_{div} curve in figure 8 is actually remarkably similar in shape to that in figures 9 and 10. Both are similarly unsymmetric about $K = -2$. Also, there are two small glitches in the regular region of every $\tilde{h}_{\text{vN}}$ curve at $K = -2$ and $K = -3$. Corresponding glitches

are just visible in the curve of figure 8. These are the result of exact periodic orbits of low periodicity (a 4-cycle for $K = -2$ and a 3-cycle for $K = -3$) which considerably reduce the classical measure $h_{\rm div}$ and are picked up by the quantum entropy measure $\tilde{h}_{\rm vN}$. These similarities imply that $\tilde{h}_{\rm vN}$ is unlike $h_{\rm KS}$ in that it is sensitive to structures (islands, periodic orbits etc.) in classical phase space.

The correspondence theory of Zurek and Paz, can be extended to account for this. The rate of vN entropy increase for a quantum system coupled to an environment is determined by the positive Lyapunov exponents (or, equivalently, the KS entropy) of the corresponding classical system because a phase space patch in the corresponding classical system stretches at an *exponential* rate if the dynamics are chaotic. Similarly, if the classical dynamics are regular, the patch will stretch *algebraically* and the rate of vN entropy increase in the corresponding quantum system will be determined by the divergence measure defined in Eq. (68).

The smooth transition from chaotic to regular dynamics in the quantum system is thus due to the peculiar nature of the quantum entropy measure: $\tilde{h}_{\rm vN}$ corresponds to $h_{\rm KS}$ in chaotic regions and $h_{\rm div}$ in regular regions making it a much more *general* measure of dynamics than either of its classical counterparts.

9.4. Quantum-classical correspondence

Since the correspondence conjecture discussed in the previous chapter was suggested for specifically chaotic motion we now look at a range of K values for which the classical KS entropy is positive *i.e.* $K \leq -4$ and $K \geq 0$. Figure 11 shows plots of the classical KS entropy of figure 6 against the corresponding plateaux of vN entropy production rates of figure 9. Similarly in figure 12, classical entropies are plotted against the quantum entropies in figure 10, this time with a higher Hilbert space dimension.

All the plots show a *linear* relationship between $h_{\rm KS}$ and $\tilde{h}_{\rm vN}$ in a chaotic region of the GCM. The linearity of the curves in figure 9 begins to break down for higher K due to saturation. This is somewhat rectified by using a higher D as shown in figure 10. In both figures there is a marked difference between the left hand ($K \leq -4$) and right hand ($K \geq 0$) curves. This is due to the relative strength of the perturbing environment. Since the environment contributes to the overall entropy increase of the quantum system, only if $\varepsilon_{\rm var} \ll K$ will the *major* entropy contribution to $\tilde{h}_{\rm vN}$ come from the chaotic dynamics of the GCM. Thus, even though classically

$$h_{\rm KS}(|K|) = h_{\rm KS}(-|K| - 4), \tag{86}$$

this is not the case for the corresponding quantum entropy measure, $\tilde{h}_{\rm vN}$, when $|K|$ is small.

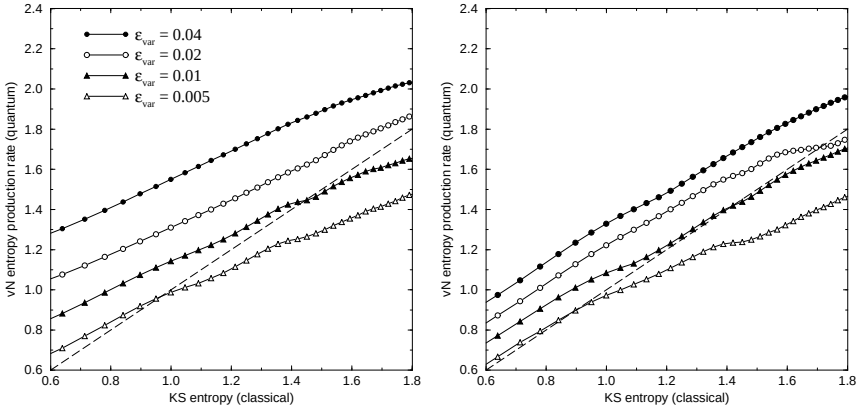

(a) $K \leq -4$ (b) $K \geq 0$

Fig. 11. Quantum-classical correspondence for the GCM: $D = 256$

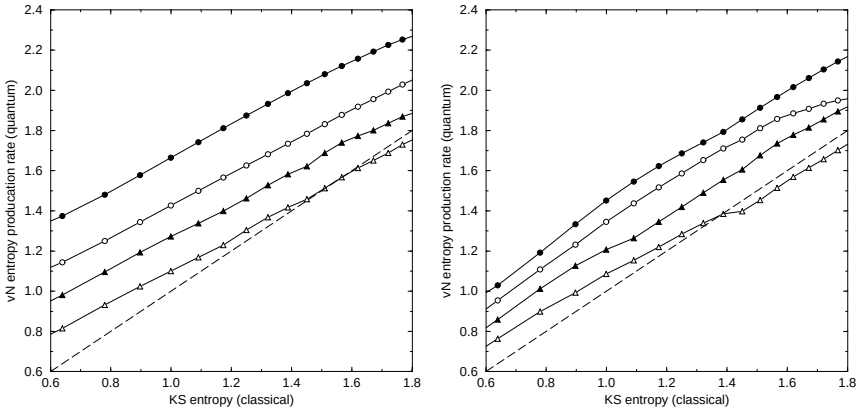

(a) $K \leq -4$ (b) $K \geq 0$

Fig. 12. Quantum-classical correspondence for the GCM: $D = 512$ (key is the same as above)

The quantum-classical correspondence is clearly dependent on both the perturbation strength of the environment and the size of the Hilbert space, *i.e.*

$$\tilde{h}_{\mathrm{vN}} = A h_{\mathrm{KS}} + c, \tag{87}$$

where $A = A(D, \varepsilon_{\mathrm{var}})$ and $c = c(D, \varepsilon_{\mathrm{var}})$. Thus, in line with Eq. (56), keeping $\varepsilon_{\mathrm{var}}$ and D constant for each curve reveals that the vN production rates are dictated by the chaotic dynamics of the GCM and *not* the environment.

The conjecture of Zurek and Paz states that for a system weakly coupled to an environment and fulfilling Eq. (58), the environmental coupling

strength does *not* appear in Eq. (57), and only helps to determine t_d, *i.e.* *when* this formula becomes valid [84]. Our work on the GCM may be used to test this conjecture.

The results in this section clearly give numerical support for the basic conjecture, but with two significant modifications:

1. The vN entropy production rate is *not* equal to the classical KS entropy, but there is in fact a *linear* relationship over a range of K values.

2. The relationship is very much *dependent* on the strength of the coupling environment. This is intuitively satisfying since the ultimate source of quantum entropy production is the environmental coupling.

9.5. Conclusions

In this section we have investigated both the regular and chaotic dynamics of the generalised cat map (GCM) in classical and quantum mechanics. We have demonstrated that there is a linear relationship between the von Neumann entropy production rate in the quantum GCM interacting with an environment and the Kolmogorov–Sinai entropy which characterises the chaotic dynamics of its classical counterpart. Regarding the regular dynamics of the GCM, we have also shown a qualitative relationship between the quantum entropy measure and a corresponding classical pseudo–entropy divergence measure of our own construction.

The strength of our approach to quantum–classical correspondence of chaotic dynamics lies in observing a *range* of results. It is not the entropy measure at a specific value of the chaos parameter K that characterises the dynamics, rather it is the *change* in entropy over a range of K values.

10. Summary

In order to see the robustness of the conclusions for the kicked rotator when a different environment is used, we coupled its momentum to the position variables of a bath of harmonic oscillators (see figure 13). Our conclusions remain unchanged [25], *i.e.* when there is the rate of change of von Neumann entropy is lineary proportional to the KS entropy.

Our approach using, entropies for both classical and quantum systems (coupled to an environment), gives a satisfying correspondence between classical and quantum systems. It is not strictly tied to semi-classical arguments, although the quantative correspondence improves in the semi-classical regime. The depth and value of our approach can be seen from noting that a range of environments lead to the same conclusions.

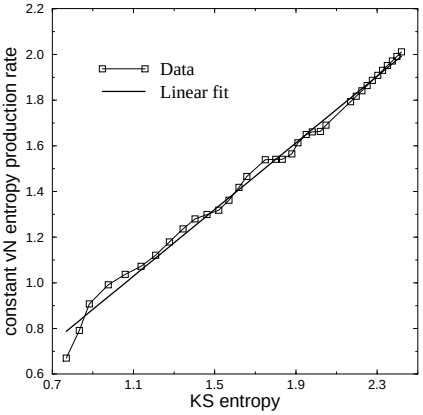

Fig. 13. The constant entropy production rate plotted against the corresponding local KS entropy. The functional relationship is $dS/dt \approx 0.7295\, h_{\mathrm{KS}} + 0.2265$

Paul A. Miller would like to thank the King's College London Association (KCLA) for a postgraduate studentship and Raphael Zarum acknowledges support from the EPSRC.

REFERENCES

[1] M. Tabor, *Chaos and Integrability in Nonlinear Dynamics : An Introduction*, Wiley, New York 1989.

[2] A.J. Lichtenberg, M.A. Lieberman, *Regular and Chaotic Motion*, Springer–Verlag, Berlin 1992.

[3] G. Iooss, R.H.G. Helleman, R. Stora, eds. *Chaotic Behaviour of Deterministic Systems*, Les Houches Lectures, Session XXXVI, North Holland, Amsterdam, 1981.

[4] L.E. Reichl, *The Transition to Chaos in Conservative Classical Systems: Quantum Manifestations*, Springer–Verlag, New York 1992.

[5] M.C. Gutzwiller, *Chaos in Classical and Quantum Mechanics*, Springer–Verlag, Berlin 1990.

[6] A.M. Ozorio de Almeida, *Hamiltonian Systems: Chaos and Quantization*, Cambridge University Press, New York 1988.

[7] G. Casati, B.V. Chirikov, *Quantum Chaos*, Cambridge University Press, 1995.

[8] M.J. Giannoni, A. Voros, J. Zinn-Justin, eds. *Chaos and Quantum Physics*, Les Houches Lectures Session LII, North Holland, Amsterdam 1991.

[9] F. Haake, *Quantum Signatures of Chaos*, Springer–Verlag, New York 1990.

[10] J.J. Sakurai, *Modern Quantum Mechanics*, Addison–Wesley Publishing Company, Reading, Massachusetts, 1994

[11] W.H. Zurek, J.P. Paz, *Phys. Rev. Lett.* **72**, 2508 (1994); G. Casati, B.V. Chirikov, *Phys. Rev. Lett.* **75**, 350 (1995); W.H. Zurek, J.P. Paz, *Phys. Rev. Lett.* **75**, 351 (1995).

[12] W.H. Zurek, J.P. Paz, *Physica D* **83**, 300 (1995).

[13] S. Habib, K. Shizume, W.H. Zurek, *Phys. Rev. Lett.* **80**, 4361 (1998).

[14] L.E. Ballentine, Y. Yang, J.P. Zibin, *Phys. Rev.* **A50**, 2854 (1994); B.S. Helmkamp, D.A. Browne, *Phys. Rev.* **E49**, 1831 (1994); R.F. Fox, T.C. Elston, *Phys. Rev.* **E49**, 3683 (1994); *Phys. Rev.* **E50**, 2553 (1994).

[15] W.H. Zurek, in the proceedings of Nobel Symposium 104, *Physica Scripta*, 1998 in press; e-print *quant-ph/9802054*.

[16] A.R. Kolovsky, *Europhys. Lett.* **27**, No 2, 79 (1994).

[17] W.H. Zurek, *Prog. Theor. Phys.* **89**, 281 (1993), and references therein.

[18] D. Giulini, E. Joos, C. Kiefer, J. Kupsch, I.O. Stamatescu, H.D. Zeh, *Decoherence and the Appearance of a Classical World in Quantum Theory*, Springer–Verlag, Berlin Heidelberg 1996, and references therein; W.H. Zurek, *Prog. Theor. Phys.* **89**, 281 (1993).

[19] W.H. Zurek, S. Habib, J.P. Paz, *Phys. Rev. Lett.* **70**, 1187 (1993).

[20] B.L. Hu, J.P. Paz, Y. Zhang, *Phys. Rev.* **D45**, 2843 (1992); *Phys. Rev.* **D47**, 1576 (1993).

[21] Y.B. Pesin, *Russ. Math. Surveys* **32**, 55 (1977).

[22] A. Farini, S. Boccaletti, F.T. Arrechi, *Phys. Rev.* **E53**, 4447 (1996).

[23] P.A. Miller, S. Sarkar, *Phys. Rev.* **E** (1998), accepted for publication.

[24] R. Feynman, F. Vernon, *Ann. Phys.* (N.Y.) **24**, 118 (1963).

[25] P.A. Miller, S. Sarkar, Entropy production, dynamical localization and criteria for quantum chaos in the open quantum kicked rotor, submitted to *Nonlinearity*, 1998.

[26] S. Sarkar, J.S. Satchell, *Physica D* **29**, 343 (1988).

[27] E. Ott, T.M. Antonsen Jr, J.D. Hanson, *Phys. Rev. Lett.* **53**, 2187 (1984).

[28] P.S. de Laplace, *A Philosophical Essay on Probabilities,* Translated by F. W. Truscott and F. L. Emory, Dover, New York 1951.

[29] E.N. Lorenz, *J. Atmos. Sci.* **20**, 130 (1963).

[30] J. Gleick, *Chaos: Making a New Science* , Viking Penguin, New York 1987, p.322.

[31] G. Iooss, R.H.G. Hellman, R. Stora (editors) , *Chaotic Behaviour in Deterministic Systems, Les Houches XXXVI* North-Holland, Amsterdam 1983.

[32] R.L. Devaney, *An Introduction to Chaotic Dynamical Systems*, Benjamin–Cummings, Menlo Park, CA, 1986.

[33] R.C. Hilborn, *Chaos and Nonlinear Dynamics: An Introduction for Scientists and Engineers*, Oxford University Press, New York 1994.

[34] G. Casati, B.V. Chirikov, F. Izraelev, J. Ford, eds., G. Casati and J. Ford, *Lecture Notes in Physics*, Springer, **93**, 334 (1979).

[35] G. Casati, I. Guarneri, D.L. Shepelyansky, *IEEE J. Quantum Electron.* **24**, 1420 (1988); S. Fishman, *Physica Scripta* **40**, 416 (1989); G. Casati, *Physica Scripta* **T39**, 85 (1991); S. Fishman, in *Quantum Chaos — Quantum Measurement,* edited by P. Cvitanović, I. Percival and A. Wirzba , Kluwer Academic Publishers, Netherlands, 1992; N. Whelan, Y. Alhassid, A. Leviatan, *Phys. Rev. Lett.* **71**, 2208 (1993); E. Eisenberg, N. Shnerb, *Phys. Rev.* **E49**, R941 (1994); G. A. Finney, J. Geabanacloche, *Phys. Rev.* **E54**, 1449 (1996).

[36] M.V. Berry, in *Chaos and Quantum Physics*, Les Houches Lectures LII, eds., M.-J. Giannoni, A. Voros, J. Zinn-Justin, North-Holland, Amsterdam 1991.

[37] M.V. Berry, *Proc. R. Soc. London A* **413**, 183 (1987); M. V. Berry, *Physica Scripta* **40**, 335 (1989).

[38] I.C. Percival, *Adv. Chem. Phys.* **36**, 1 (1977).

[39] N. Pomphrey, *J. Phys. B* **7**, 1909 (1974); D.W. Noid, M.L. Koszykowski, M. Tabor, R.A. Marcus, *J. Chem. Phys.* **72**, 6169 (1980).

[40] O. Bohigas, in *Chaos and Quantum Physics*, Les Houches LII, eds., M.-J. Giannoni, A. Voros and J. Zinn-Justin, North-Holland, Amsterdam 1991.

[41] M.C. Gutzwiller, *Chaos in Classical and Quantum Mechanics*, Springer–Verlag, New York 1990.

[42] E.J. Heller, in *Chaos and Quantum Physics*, Les Houches LII, eds., M.-J. Giannoni, A. Voros and J. Zinn-Justinn, North-Holland, Amsterdam 1991.

[43] G.J. Chaitin, *Information, Randomness & Incompleteness: Papers on Algorithmic Information Theory*, World Scientific, Singapore 1987.

[44] J. Ford, in *Chaotic Dynamics and Fractals,* eds., M. F. Barnsley and S. G. Demko Academic Press, New York 1985.

[45] V.M. Alekseev, M.V. Yakobson, *Phys. Rep.* **75**, 287 (1981); B.V. Chirikov, F.M. Izrailev, D.L. Shepelyansky, *Physica D* **33**, 77 (1988).

[46] J. Ford, in *The New Physics,* ed., P.C.W. Davies, Cambridge University Press, Cambridge 1989.

[47] J. Ford, G. Mantica, G. Ristow, *Physica D* **50**, 493 (1991); J. Ford, M. Ilg, *Phys. Rev.* **A45**, 6165 (1992); J. Ford, G. Mantica, *Am. J. Phys.* **60**, 1086 (1992).

[48] D. Giulini, E. Joos, C. Kiefer, J. Kupsch, I.-O. Stamatescu, H.D. Zeh, *Decoherence and the Appearance of a Classical World in Quantum Theory,* Springer–Verlag, Berlin Heidelberg 1996, p. 125.

[49] R. Schack, C.M. Caves, *Phys. Rev. Lett.* **71**, 525 (1993).

[50] R. Schack, G.M. D'Ariano, C.M. Caves, *Phys. Rev.* **E50**, 972 (1994).

[51] R. Schack, C.M. Caves, *Phys. Rev.* **E53**, 3257 (1996).

[52] W.H. Zurek, J.P. Paz, *Phys. Rev. Lett.* **72**, 2508 (1994).

[53] W.H. Zurek, J.P. Paz, *Physica D* **83**, 300 (1995).

[54] B.V. Chirikov, *Phys. Rep.* **52**, 263 (1979).

[55] V.I. Arnold, *Mathematical Methods in Classical Mechanics,* Springer, New York 1978.

[56] J.N. Mather, *Ergodic Theory Dyn. Syst.* **2**, 301 (1984); R.S. MacKay, I.C. Percival, *Commun. Math. Phys.* **98**, 469 (1985).

[57] J.M. Greene, *J. Math. Phys.* **20**, 1183 (1979).

[58] J.D. Meiss, *Phys. Rev.* **A34**, 2375 (1986).

[59] M. Tabor, *Chaos and Integrability in Nonlinear Dynamics: An Introduction*, Wiley, New York 1989.

[60] C. Beck, F. Schögl, *Thermodynamics of Chaotic Systems: An Introduction*, Cambridge University Press, 1993.

[61] V.I. Oseledec, *Trans. Moscow Math. Soc.* **19**, 197 (1968);
J.P. Eckmann, D. Ruelle, *Rev. Mod. Phys.* **57**, 617 (1985).

[62] G. Benettin, L. Galgani, J.M. Strelcyn, *Phys. Rev.* **A14**, 2338 (1976).

[63] Ya.B. Pesin, *Russian Math. Surveys* **32**, 55 (1977).

[64] V.I. Arnol'd, A. Avez, *Ergodic Problems of Classical Mechanics,* Benjamin, New York 1968.

[65] T.C. Halsey, M.H. Jensen, L.P. Kadanoff, I. Procaccia, B.I. Schraiman, *Phys. Rev.* **A33**, 1141 (1986).

[66] R.V. Jensen, C.R. Myers, *Phys. Rev.* **A32**, 1222 (1985).

[67] Z. Su, R.W. Rollins, E.R. Hunt, *Phys. Rev.* **A36**, 3515 (1987).

[68] P. Martin-Löf, *J. Information and Control* **8**, 602 (1966).

[69] C. Grebogi, S.M. Hammel, J.A. Yorke, T. Sauer, *Phys. Rev. Lett.* **65**, 1527 (1990).

[70] D.K. Arrowsmith, C.M. Place, *An introduction to Dynamical Systems*, Cambridge University Press, Cambridge 1990.

[71] Y. Kifer, *Random Perturbations of Dynamical Systems*, Birkhäuser, Boston 1988.

[72] K. Nakamura, *Quantum Chaos: A New Paradigm of Nonlinear Dynamics*, Cambridge University Press, Cambridge 1993.

[73] G.M. Zaslavsky, *Chaos in Dynamic Systems,* Harwood Academic Publishers, 1984.

[74] M.V. Berry, in *New Trends in Nuclear Collective Dynamics,* edited by Y. Abe, H. Horiuchi, and K. Matsuyanagi , Springer, Berlin 1992.

[75] C.M. Caves, *Phys. Rev.* **E47**, 4010 (1993).

[76] R. Schack, C.M. Caves, *Phys. Rev.* **E53**, 3387 (1996).

[77] R. Landauer, *IBM, J. Res. Devel.* **5**, 183 (1961).

[78] C.M. Caves, in *Complexity, Entropy and the Physics of Information,* edited by W. H. Zurek, Addison–Wesley, Redwood City, CA, 1990, p. 91.

[79] E.T. Jaynes, in *Papers on Probability, Statistics, and Statistical Physics,* edited by R. D. Rosenkrantz, Kluwer, Dordrecht 1983.

[80] M. Saraceno, *Ann. Phys.* **199**, 37 (1990).

[81] J.J. Sakurai, *Modern Quantum Mechanics,* Addison–Wesley, New York 1994.
[82] W.H. Zurek, S. Habib, J.P. Paz, *Phys. Rev. Lett.* **70**, 1187 (1993).
[83] W.H. Zurek, *Prog. Theor. Phys.* **89**, 281 (1993).
[84] W.H. Zurek, to be published [e-print quant-ph/9802054].
[85] I.C. Percival, F. Vivaldi, *Physica D* **27**, 373 (1987).
[86] J.P. Keating, *Nonlinearity* **4**, 309 (1991).
[87] F. Benatti, H. Harnhofer, G.L. Sewell, *Lett. Math. Phys.* **21**, 157 (1991).
[88] A. Lakshminarayan, *Phys. Lett.* **A192**, 345 (1994).
[89] A. Lakshminarayan, N.L. Balazs, *Chaos, Solitons & Fractals* **5**, 1169 (1995).
[90] M.V. Berry, N.L. Balazs, M. Tabor, A. Voros, *Ann. Phys.* (N.Y.) **122**, 26 (1979).
[91] R. Zarum, S. Sarkar, *Phys. Rev.* **E57**, 5467 (1998).